Photochemical & Photobiological Sciences

Accepted Manuscript

This is an *Accepted Manuscript*, which has been through the Royal Society of Chemistry peer review process and has been accepted for publication.

Accepted Manuscripts are published online shortly after acceptance, before technical editing, formatting and proof reading. Using this free service, authors can make their results available to the community, in citable form, before we publish the edited article. We will replace this *Accepted Manuscript* with the edited and formatted *Advance Article* as soon as it is available.

You can find more information about *Accepted Manuscripts* in the Information for Authors.

Please note that technical editing may introduce minor changes to the text and/or graphics, which may alter content. The journal's standard Terms & Conditions and the Ethical guidelines still apply. In no event shall the Royal Society of Chemistry be held responsible for any errors or omissions in this *Accepted Manuscript* or any consequences arising from the use of any information it contains.

ROYAL SOCIETY OF CHEMISTRY

www.rsc.org/pps

Applications of phototransformable fluorescent proteins for tracking dynamics of cellular components

Ina Nemet, Philip Ropelewski, and Yoshikazu Imanishi#

Department of Pharmacology, Case Western Reserve University, Cleveland OH 44106.

#Corresponding author address: Department of Pharmacology, 10900 Euclid Avenue, Cleveland, OH 44106, Tel: +1 216 368 2586 Email: yoshikazu.imanishi@case.edu

Abstract

In the past few decades, fluorescent proteins have revolutionized the field of cell biology. Phototransformable fluorescent proteins are capable of changing their excitation and emission spectra after being exposed to specific wavelength(s) of light. The majority of phototransformable fluorescent proteins originated from marine organisms. Genetic engineering of these proteins has made available many choices for different colors, modes of conversion, and other biophysical properties. Their phototransformative property has allowed highlighting and tracking of subpopulations of cells, organelles, and proteins in living systems. Furthermore, phototransformable fluorescent proteins paved new ways for superresolution fluorescence microscopy and optogenetics manipulation of proteins. One of the major advantages of phototransformable fluorescent proteins is their applicability for visualizing newly synthesized proteins that are *en route* to their final destinations. In this manuscript, we will discuss biological applications of phototransformable fluorescent proteins with special emphasis on the applications of tracking membrane proteins in vertebrate photoreceptor cells.[1]

[1] Parts of the data in this paper were presented during the 16th International Congress on Photobiology held in Cordoba, Argentina, in September (8th - 12th), 2014.

Introduction

Beginning with the discovery and molecular cloning of the green fluorescent protein (GFP), fluorescent proteins (FPs) have contributed to the advances in biomedical sciences by allowing genetic and noninvasive labeling of cells, organelles, and proteins. Further improvements in spatial and temporal labeling of proteins and biological structures were accomplished through the use of a unique class of fluorescent proteins: phototransformable fluorescent proteins (PtFPs). PtFPs are capable of changing their fluorescence excitation and emission spectra after irradiation by unique wavelength(s) of light. PtFPs that change from one fluorescent state to another are called photoconvertible fluorescent proteins (PcFPs), whereas PtFPs that are irreversibly activated from a non-fluorescent (dark) state to an emitting state are specifically called photoactivatable fluorescent proteins (PaFPs).[1] The unique photoconversion property was first discovered in what was identified as a GFP homolog, Kaede,[1, 2] which turned out to be a green-to-red PcFP. The first PaFP, photoactivatable GFP (paGFP), was developed through a site directed mutagenesis study of GFP.[2] Since the discovery of Kaede and paGFP, a number of PtFPs with distinct fluorescence properties were found and engineered. For the majority of PtFPs, the mechanism of phototransformation involves light-induced cleavage of the protein backbone and formation of a Cα-Cβ double bond in chromophore's histidine[3, 4] or in the oxazole ring formed during chromophore maturation[5] (Fig 1A and B, respectively). In some proteins, light-induced decarboxylation of glutamate residue close to the chromophore is the cause of photoconversion[6] or photoactivation (Fig. 1C).[7] While those types of phototransformation are irreversible, light-induced conformational rearrangements of the chromophore and its environment are reversible and allow the protein to be switched between a fluorescent on-state and a non-fluorescent off-state (Fig. 1 D).[8, 9] These reversibly transformable

FPs are known as photoswitchable fluorescent proteins (PsFPs). Furthermore, a class of PtFPs that combines the properties of reversibly photoswitchable and irreversibly photoactivatable fluorescent proteins are categorized as biphotochromic FPs.[10, 11] For a comprehensive overview on PtFPs and their characteristics, we suggest the readers to refer to several excellent reviews published recently.[12-14] In this review, we will discuss how these distinct photochemical properties of PtFPs contributed to the development of different methods for labeling cellular components and understanding the dynamics of cells, organelles, and proteins (summarized in Table 1 and Fig. 2).

Among the biological applications, PtFPs are particularly suited for studying protein movement in individual cells and between different subcellular organelles (Fig. 2). Traditionally, vertebrate rod photoreceptor cells have served as valuable models for the studies of vectorial protein trafficking.[15] Photoreceptors have been attractive models because of their polarized structure and highly active protein trafficking which enables rapid renewal of the photosensitive outer segment (OS).[16] Until the advent of PtFPs, the technique to visualize protein trafficking in native rods, however, had been limited to autoradiography of radiolabeled proteins.[15] The radiolabeling method is not suitable for monitoring the trafficking of specific protein(s), as labeling occurs randomly for any synthesized proteins. In addition, it is impossible to monitor protein trafficking in living cells and tissues using radiolabeling due to the requirement of chemical fixation. These problems are circumvented by the use of PtFPs fused to proteins of interest, since imaging can occur *in vivo*, and high contrast can be obtained for either most recently synthesized proteins or subpopulation of proteins in cellular organelles. In this review, we will discuss the recent advances and possible future applications of the phototransformable

technology to visualize trafficking of proteins and renewal of cellular organelles, with special emphasis on the studies of rod photoreceptor cells.

Tracking of Cells

PtFPs offer advantages in studying cell fate, cell migration, tissue development and regeneration. A common technique involves expression of a PcFP in cells of interest followed by photoconversion of a single cell or a subpopulation of cells in specific location of tissue and animals (Fig 2A). Traditional FPs did not allow such localization-dependent subpopulation labeling, making it difficult to discriminate the cells from different origins. For example, green-to-red photoconvertible Kaede was one of the earliest PcFPs to be utilized for specific cell tracking.[17] In this case, red fluorescent (photoconverted) cells are followed *via* time lapse imaging. Such approach has been used for monitoring the development of neural networks in wide range of vertebrate species from teleost fish[18] to mammals.[19] In mouse neonatal brain, for example, usage of Kaede facilitated monitoring the movement of a progenitor cell from one compartment to another (from ventricular zone to subventricular zone) while permitting visualization of the division of the same cell. Discrimination of individual daughter cells was also possible by photoconverting one of the daughter cells shortly after mitosis. This specific photoconversion allowed tracking the fates of those cells which eventually migrated into different directions.[19] Kikume Green-to-Red PcFP (KikGR) is highly suited for cell tracking due to its brighter fluorescence and more complete photoconversion compared to other PtFPs such as Kaede, paGFP, and cyan-to-green PcFP PS-CFP2, and thus was used for tracking neural crest cells in chick embryos[20, 21] as well as monitoring cell fates in different organs of mouse embryos.[22] Other PtFPs such as EosFP (green-to-red PcFP) were successfully used for monitoring the division and lineage of vertebrate embryonic cells for a period of up to two weeks.[23] The cell tracking capability of PcFPs has also aided studies of tissue regeneration. In a zebrafish model, Kaede was used to determine how osteoblasts dedifferentiate and migrate to

damaged sites where they can regenerate bones.[24] Likewise, cell movement associated with fin regeneration was studied using a new model called PhOTO zebrafish ubiquitously expressing green-to-red Dendra2 PcFP.[25]

While the above applications are concerned about vertebrates, PcFPs have also been expressed in invertebrates to understand their developmental processes. For example, Kaede was used to label subpopulations of cells and track their divisions and eventual fate in a plankton species *Oikopleura dioica.*[26] In this system Kaede photoconversion allowed identification of three cell types that exhibit long distance migration during development: a multi nucleated oral gland, endodermal strand cells and two subchordal cell precursors. PcFPs are not the only class of PtFPs used for monitoring cell dynamics. PaFPs can also be used for such approach as demonstrated by fusing paGFP to alpha-tubulin for monitoring mesoderm migration in the early embryonic development of *Drosophila melanogaster*.[27]

In addition to tracking the fates of cells, PcFPs can be used for determining the birthdates of cells. Accurate determination of birthdates, however, is only possible if the PcFP is expressed under a promoter which triggers expression after the last cell division. After photoconversion, early-born cells contain converted PcFP as well as non-converted protein (newly synthesized after conversion), while late-born cells, which were not present at the time of photoconversion, contain only non-converted PcFP. This approach, also known as birthdating analysis by photoconverted fluorescent protein tracing *in vivo* (BAPTI), was used to distinguish early-born from late-born trigeminal sensory neurons in live zebrafish embryos by expressing Kaede under the *huc* promoter.[28] BAPTI was further combined with an additional method to mark a subpopulation of cells with enhanced GFP (EGFP) which was expressed under the control of *cis*-regulatory region of genes, such as TrpA1 and p2x3b. This combined method was coined

BAPTISM (BAPTI plus subpopulation marker) and allows discriminating the differentiation status of the early- and late-born cells. BAPTISM unraveled that late-born trigeminal sensory neurons, unlike early-born ones, do not form chemosensory neurons expressing the ion channel TrpA1b. [28]

The photoconversion approach was harnessed for tracking immune cells as well.[29, 30] For example, Kaede was used for tracking the destiny of different leukocyte populations in skin. After exposure to photoconverting UV light, $CD4^{+}CD25^{-}$ non-Treg and CD4+CD25+ nTreg leukocytes (labeled in red) moved from the skin into draining lymph nodes at steady state.[30] Applying two-photon excitation[31] for photoconversion allowed the use of infrared light to photoactivate cells buried deep within tissues in a three-dimensionally confined pattern without highlighting undesired cells or causing phototoxicity in the light path. Use of two-photon excitation was effective in labeling subpopulation of follicular B cells and subsequent monitoring of their dissemination between spatially separated lymphoid organs within a living adult mouse.[32]

The mechanism of host-pathogen cell-cell interactions have also been clarified from the use of PcFPs. A green-to-red PcFP monomeric KikGR (mKikGR) was expressed in *Leishmania major*, a pathogenic species of protist, in order to study pathogen reaction to the immune response.[33] Biochemical analysis indicated that the activity of ribosome promoter can be used as proxy for metabolic and proliferative activities of the parasitic cells. Thus, the expression of mKikGR was regulated by the ribosome promoter, and the promoter activity was determined as the recovery of fluorescence originating from newly synthesized (non-photoconverted) mKikGR which can be visualized after photoconversion. By utilizing this fluorescence recovery after conversion (FRAC) method, host-parasite interaction was studied. In the presence of nitric oxide

produced by the immune system, the replacement of red (old) protein with green (new) protein was slowed and initial burst in protein synthesis was absent, suggesting the decrease of the parasite's metabolism due to nitric oxide-mediated oxidative stress. Thus, the photoconversion technique unraveled a possible defense mechanism against this pathogenic species, and provided an opportunity to further dissect how the immune system affects pathogen metabolism.

Studies of organelle dynamics.

Subcellular organelles continuously exchange their contents and are highly dynamic. PtFPs can be used to specifically label individual subcellular organelles, and improve the method of visualizing organelle dynamics. In these applications, PtFPs are targeted to specific organelles through fusion with specific targeting signal or protein domain (Fig. 2B). For instance, mitochondria are highly dynamic organelles. Their fission and fusion play critical roles in maintaining their integrity and connectivity. Fusing mitochondrial matrix and outer membrane targeting sequences to paGFP allowed tracking mitochondria dynamics in cultured mammalian cells (Fig 2B-1).[34] After photoactivation of a single mitochondrion or small group of mitochondria, redistribution and dilution of activated mitochondria protein-paGFP can be monitored and quantified in real time.[35, 36] This methodology was applied on different cell types and helped unravel the mechanisms of mitochondrial morphogenesis[37] and fission[38] as well as the role of mitochondrial fusion in activating apoptosis.[35, 39] In adult rat cardiomyocytes preparation, the method revealed additional modes of inter-mitochondrial interactions, called "kissing" and "nanotunneling".[40] These transient interactions have important implications for rapid signaling among mitochondria and for metabolic regulation in the heart.[40] Prior to the

advent of PtFPs, the mitochondria fusions were usually studied by fusing two haploid cells whose mitochondria were labeled with two different fluorescent probes (e.g. GFP and RFP). Fusion of two differently labeled mitochondria leads to mixing of fluorescence probes. Such experimental paradigm requires two haploid cells to be fused through treatment by virus or polyethylene glycol, which may disrupt membrane physiology and was not applicable to intact tissues or animals.[41-44] To improve the method for monitoring mitochondria dynamics *in vivo*, a transgenic mouse line was generated to ubiquitously express mitochondrially localized version of Dendra2, which was successfully used to monitor mitochondrial fusion events in cultured cells as well as tissues such as skeletal muscle.[45] Similar to mitochondria, the study of paGFP fused to a lysosomal membrane protein lgp120 demonstrated a surprisingly dynamic exchange of proteins among lysosomes.[2] Peroxisomal targeting sequence was also fused to mEos2, an improved version of EosFP engineered to be bright/photostable, monomeric and mature efficiently at 37 ˚C.[46] A transgenic mouse model was created to label subpopulation of peroxisomes specifically in oligodendrocytes.[47] In theory, such a model is useful for tracking the fate of individual peroxisomes and comparing healthy and disease model mice with afflicted peroxisome functions. In addition to the study of organelles in mammalian cells, PcFPs have also contributed to the studies of plant organelle dynamics. Plastids, subcellular organelles of plants and algae specialized for manufacturing and storing nutrients and other useful compounds, have been hypothesized to exchange materials among each other.[48] In the past, studies were conducted using GFP targeted to stroma of the plastids. GFP was photobleached in one of apparently connected multiple plastids to test if GFP from the other plastids would diffuse into the bleached plastid. Although the fluorescence recovered in photobleached plastids, the single colored GFP did not allow testing where recovered GFP originated from, and thus did not prove that

recovered GFP was derived from interconnected plastids.[48, 49] The use of green-to-red photoconvertible EosFP (mEosFP) allowed testing of the interconnectivity. For this purpose mEosFP was fused to a part of plastid ferredoxin NADP(H) oxidoreductase and expressed in plant cells. Photoconversion of mEosFP in individual plastids allowed differential coloring of individual plastids.[50] This approach demonstrated that plastids do not form a network for exchanging large molecules with size equivalent to mEosFP. Thus, such absence of material exchange could be one of the bases for generating functionally diverse plasmids within a single plant cell.[50, 51] Thus, PcFPs and PaFPs are useful for the studies of protein exchange (or the lack of exchange) among different cellular compartments in plants and animals.

Dynamic processes associated with Golgi, specifically the secretory pathway, have also been successfully studied using PtFPs. Proteins of interest directly fused to paGFP can be activated at the Golgi apparatus to track fluorescence of nascent proteins without having background of pre-existing proteins (Fig 2B-2). For instance, this technique combined with multiplex confocal microscopy elucidated the trafficking route of the Amyloid Precursor Protein (APP)-paGFP fusion in murine neuronal cell line.[52] The paGFP was fused to the APP's C-terminal (Ct) tail which is cleaved off through posttranslational proteolysis. This cleavage renders APP to be amyloidogenic. To distinguish different cellular compartments occupied with APP-paGFP, the Golgi apparatus was labeled with a cyan fluorescent protein while lysosomes, early and late endosomes were labeled with a red fluorescent protein. Using cyan labeling as a guide, Golgi-APP-paGFP was photoactivated only in Golgi and followed over time. From Golgi apparatus, the photoactivated APP-paGFP was predominantly delivered to the lysosomal compartment (labeled as red), where paGFP was cleaved off and APP was processed to a shorter isoform with increased propensity of forming beta-amyloid. In addition to mammalian cells,

Golgi dynamics were also studied in plant cells. The Golgi apparatus experiences dynamic changes during the cell cycle including the new synthesis of Golgi membrane protein sialyl transferase. After photoconversion of Kaede-sialyl transferase fusion protein, newly synthesized Kaede fusion can be appreciated in green, thus allowing the rate of new protein synthesis to be measured.[53] This measure was useful to determine that the synthesis of this Golgi marker increases during the second half of the G1 phase and persists during S and G2 phases of the cell cycle.[54] This is likely a mechanism to adapt to the need for cell growth as Golgi is a critical organelle for biogenesis of cellular components.

Another organelle responsible for cell cycle regulation is the centrosome. The centrosome consists of two centrioles that reside at the microtubule organizing center (MTOC); for the majority of cell types, the centrosome is copied once per cell cycle and both the mother and daughter cell each inherit one copy of the centrosome. Kaede fused to a centrosome marker has been used to study the inheritance pattern of centioles.[55-57] In this setting, cells are photoconverted prior to cell division, so that a pair of centrioles in a single cell is red. After the first cell division, centrioles originating from the mother cell are red, while centrioles synthetized in the daughter cells are green. After the second cell division, it becomes possible to clarify which cells received the mother centriole and which received the daughter centriole (Fig 2B-3). This research design was applied to mouse neocortex, and led to a discovery that specific inheritance of mother centriole is required for the stemness and the maintenance of radial glia progenitors.[57]

The primary cilium is a subcellular organelle which plays critical sensory and signaling roles.[58] For proper ciliary signaling, dynamic exchanges of signaling components are necessary for many sensory functions but have been difficult to visualize. In the past, studies on protein

dynamics in cilia have been constrained by the limitation of the fluorescence recovery after photobleaching (FRAP) technique. With conventional FPs, one can observe fluorescent fusion protein entering the cilia after bleaching, but cannot observe protein leaving the cilia simultaneously. Instead, fusion protein consisting of PcFP can be highlighted and then tracked as it exits the cilia. By labeling a ciliary-localized protein with a PcFP, such as mEos2, it is possible to utilize low-intensity photoconversion light in place of intense photobleaching light.[59] Photoconversion beam can be focused on the cilia to proteins only in this subcellular compartment. Under this condition, proteins existing outside of the cilia at the time of photoconversion remain in green. Thus, both the import and export of ciliary proteins can be investigated through monitoring of converted and non-converted fluorescent fusion proteins (Fig. 2B-4). This technique elucidated how the ciliary exchange of smoothened, a component of Hedgehog pathway, can be modulated by different small molecules. The study revealed that cyclopamine selectively inhibits the ciliary entry whereas ciliobrevin initially inhibits the ciliary exit of smoothened fused to mEos2.[59]

Improvements of PtFPs for labeling proteins

Many first generation PcFPs (including Kaede and EosFP) form oligomers at low concentrations.[60] While oligomer formation may not be a major concern for tracking entire cells, it is a major concern when tracking individual protein components. The tendency for fluorescent proteins to form oligomers is problematic as dimeric and tetrameric complexes can alter the function or localization of the partners to which these FPs are fused to. Thus, it has been desirable to engineer PcFPs with propensity to form monomers at high concentrations (~ 100

μM). For example: a monomeric form of EosFP was successfully engineered and named mEosFP, which is suitable for localization studies.[61, 62] Dendra fluorescent proteins also have monomeric versions,[63] and similarly mKikGR[64] is a monomeric version of KikGR.[65] Likewise, PaFP (paGFP) and PsFP (Dronpa) were engineered to be monomeric.[2, 8, 66] While those monomeric versions of PtFPs have much less tendencies to form oligomers, it is crucial to note that some PcFPs may still form oligomers at high concentrations (10 - 100 μM).[10] For example, mEos2 was originally considered monomeric, but was later found to form dimers at concentrations higher than 20 μM.[46, 67, 68] An improvement of mEos2 lead to the design of mEos3.1 and 3.2, which barely oligomerize at the concentrations higher than 200 μM.[67] Other than oligomerization status, critical limitation for protein labeling is that the majority of PcFPs may not quickly and fully mature in warm-blooded animals (36 – 37 ˚C). To overcome this limitation, efforts were made to improve the maturation rate of PcFPs at high temperature as exemplified by Dendra2[69, 70] and mEos proteins (mEos2, 3.1 and 3.2).[46, 67]

While substantial improvements have been made to FPs to increase their viability for accurate labeling of proteins,[71, 72] an unavoidable shortcoming is their relatively large size (~25 kDa). Fusing a FP to a protein of interest may sterically hinder critical transport or localization signals, or may even compromise the function(s) of the tagged protein.[73] Furthermore, overexpression of PtFP fusion proteins may lead to undesirable dominant negative effects; even PtFPs not fused to any protein may be potentially toxic to cells.[74] In addition to the protein toxicity, the activating/excitation light source of the PtFP could cause photodamage to the cell and induce artifacts or abnormal cell function.[75] Thus, control experiments should be carefully designed in order to verify that neither the light source nor the PtFP being expressed is affecting

protein function, localization, or cell health, any of which would negatively impact proper interpretation of the results.[76]

Tracking proteins in the endolysosomal and secretory pathways.

PtFPs have been effectively used to study the process of protein endocytosis and exocytosis. G protein-coupled receptors (GPCRs) are one of the most important classes of receptors, and are the targets of a large number of pharmaceuticals.[77] Agonist stimulation of GPCRs often causes their internalization through endocytosis, resulting in their desensitization. Internalized GPCRs may be recycled back to the plasma membrane, or delivered to and degraded by lysosomes. Traditionally, trafficking of proteins was studied by fusing them to a FPs in combination with FRAP methodologies; however, in the case of recycling GPCRs, it is impossible to discriminate between receptors that have been recycled and have returned to the plasma membrane from newly synthesized receptors arriving from the secretory pathway. In these cases, conventional recycling assays such as biotin-labeling of cell surface receptors followed by immune-precipitation should be used. Fates of GPCRs after internalization can be effectively determined by using GPCR-PcFP fusion protein.[78] After agonist stimulation, endosomes containing GPCR-PcFP fusion protein can be locally photoconverted and its fate can be monitored over time. Using this methodology, it was demonstrated that corticotropin-releasing factor receptor type 1 belongs to the family of recycling GPCRs.[78]

PtFPs also contributed to the understanding of insulin secretion. Tracking individual insulin granules using traditional FPs has been challenging due to a large number of granules which are simultaneously secreted. Thus the conventional technique was more accessible to

readily releasable pool of granules which are proximately located to the plasma membrane and do not travel long distances.[79-81] Fusing granule membrane (phogrin) or cargo (neuropeptide Y) protein with paGFP or Dendra2 followed by photoactivation or photoconversion, respectively, allows reliable long-distance tracking of individual granules through the cytoplasm until their fusion with the plasma membrane and subsequent insulin release. This method revealed that the rate of granule movement after starvation and subsequent glucose stimulation was higher when cells were pre-incubated with a higher concentration of glucose. This knowledge may partly explain how defects in pancreatic insulin secretion occur in diabetic patients.[82] Such a method employing a paGFP or PcFP may also elucidate the poorly understood mechanisms of insulin granule fission and fusion.[82]

Monitoring of soluble proteins and their surrounding microenvironment

Using conventional FPs, diffusion of fusion proteins has been traditionally assessed by FRAP and florescent loss in photobleaching (FLIP) techniques.[83] Although successful in determining diffusion coefficient of multiple proteins, these techniques require relatively long and high-energy illumination of specific region of the cell and they cannot be utilized to analyze either fast diffusions or diffusion of proteins buried deep in a tissue. They also suffer from low signal to noise ratio and production of toxic products during photobleaching. Because of the use of short and low-energy illumination required for photoconversion/photoactivation, PtFPs can overcome those disadvantages and be used in determining proteins diffusion coefficients through measurement of fluorescence decay after photoactivation (FDAP), in which emigration of PtFP fusion proteins results in decreased fluorescence from photoactivated/photoconverted area (Fig.

2C). This FDAP approach was harnessed to understand the diffusion of cytoplasmic proteins. One example of such approach is measuring the diffusion dynamics of a transcription factor Oct4 in mouse embryos. The study revealed that Oct4-paGFP diffusion kinetics depends on its interaction with methyltransferase ERG-associated protein with SET domain.[84] The Oct4 kinetics is more critical than its expression level to determine the developmental cell lineage pattering in early mouse embryos.[85] FDAP approach, when combined with two-photon infrared excitation, improve the accuracy of the experiments by enabling 3-dimensionally confined photoactivation of PtFPs. Thus, for example, two-photon excitation of paGFP fused β-actin allowed 3D-restricted highlighting of F-actin and monitoring its movement in live neurons, revealing the three pools of F-actin underlie spine structure and plasticity.[86] Moreover, measuring the diffusion of paGFP in different regions of highly polarized photoreceptor cells including OS and connecting cilium (CC) provided direct evidence that CC obstruct soluble proteins movements from the cell body to the OS, but it does not pose a major barrier to protein movement. Axial diffusion of soluble proteins within the primary cilium, on the other hand, was 50-fold slower than predicted.[87] In addition, a model was provided to explain the distribution of soluble proteins in distinct cytoplasmic volumes of rod OS and inner segment (IS). In this model, steric hindrance leads to reduction in the effective volume for larger molecules to diffuse in, leading to size dependent exclusion of soluble proteins from the OS. This model was supported by a study monitoring the steady-state distributions of GFP monomer and concatemers, demonstrating the size dependent exclusion of GFP concatemers from the OS. paGFP monomer and concatemers (3xpaGFP) allowed monitoring their movements from IS to OS. This photoactivation experiment provided evidence that protein flux through the ciliary transition zone was not significantly different between monomeric and paGFP concatemer, and thus size-

dependent distribution was not a result of a possible size-dependent diffusion barrier for soluble proteins at the base of the OS. While remains to be tested, this steric hindrance model may explain the expulsion of another soluble protein, arrestin, from the photoreceptor OS during dark adaptation and after its release from photoactivated rhodopsin.[88]

While the majority of the previously described applications include PcFPs and PaFPs, PsFPs provide specific advantages in understanding fast, dynamic protein exchange between different cellular compartments.[8] PcFPs and PaFPs can be highlighted only once. However, PsFP Dronpa allows reversible highlighting of the same proteins multiple times (Fig. 2D). Dronpa was introduced to study the dynamics of ERK1 translocation.[8] ERK1 fused to Dronpa is initially localized in the nucleoplasm and cytoplasm under steady state with minimal exchange between those two compartments. Upon EGF stimulation both ERK-Dronpa import and export were accelerated contradictorily to the previously proposed models of one-directional (cytosol to nucleus) ERK translocation. This study took advantage of the photochemical property of Dronpa, which allowed highlighting nuclear ERK1-Dronpa and observation of its export to cytosol. After erasing all the fluorescence in the same cell followed by highlighting cytosolic ERK1-Dronpa, its import to nucleus can be monitored in real-time. This process can be repeated multiple times for PsFPs and thus is useful to visualize dynamic import and export of proteins in the same cells over time.

In addition to monitoring protein mobility, PsFP Dronpa found another application as a sensor for viscosity of cytoplasmic volume.[89] Bright-to-dark photoswitching kinetics of the Dronpa and its Dronpa-3 mutant significantly slow down with increasing viscosity of the cytoplasmic microenvironment where the proteins are exposed. This kinetics property made these PsFPs useful tools for mapping out spatial distributions of viscosity and macromolecular

crowding in the living cells that could play important role in different cellular processes such as protein assembly, signal transductions, diffusion of different (macro)molecules or nuclear envelope function and chromatin localization as demonstrated for cell nucleus by histone-Dronpa-3 fusion protein.[89]

Diffusion of membrane proteins.

Application of PtFPs also gave new insights into diffusion of proteins across compartmentalized membranes. Two-photon excitation allowed production of very small volume of photoactivated GPCR rhodopsin-paGFP. Tracking rhodopsin-paGFP movement after the photoactivation demonstrated that its lateral diffusion is highly heterogeneous within rod photoreceptor disks and allowed examination of the influence of the membrane geometry on GPCR mobility.[90] Single-particle tracking in live cells also allowed examination of the impact of the heterogeneities on individual protein movement.[91-93] For single-particle tracking, proteins are labeled with gold beads [94] or FPs [92]. For conventional single-particle tracking, only small number of molecules can be labelled and tracked in one experiment, because those particles need to be sufficiently separated by a distance more than a diffraction limit of light. To improve imaging resolution and monitor the trajectories of many particles in one experimental session, photoactivated localization microscopy (PALM) was used for single-particle tracking in a new method termed sptPALM. This technique allows reconstruction of the molecular trajectories by connecting the positions of a photoactivated protein from consecutive frames. As this method allows iterative processes of photoactivating, imaging and bleaching molecules in the same cells, unlike traditional approaches where single molecules are imaged until bleached only once in the sample.

Thus sptPALM, is capable of visualizing multiple single molecule-trajectories in the same small area. When HIV-1 protein Gag or vesicular stomatitis virus glycoprotein (VSVG) were fused to EosFP and expressed in COS7 cells, several orders of magnitude more trajectories per cell were obtained in comparison with conventional single-particle tracking making this method suitable for obtaining spatially resolved information about membrane protein dynamics.[95] Trajectories of two distinct protein populations, one fused to monomeric photoactivable red fluorescent protein (paTagRFP) and another to paGFP, were compared in the same cell. The trajectories of epidermal growth factor receptor, VSVG and transferrin receptor were compared to that of clathrin light chain (CLC), marker for clathrin-coated pits. This experiment demonstrated that epidermal growth factor and transferrin receptors, but not VSVG, move together with CLC-positive plasma membrane domain. The experiment also suggested that a subpopulation of epidermal growth factor and transferrin receptors continuously localize in CLC-positive plasma membrane domains both in the presence and absence of ligand activation[96]

Application of PtFPs for studying protein-protein interactions.

PtFPs can also be used for studying protein-protein interactions and determining the oligomerization status of proteins through the use of the Förster resonance energy transfer (FRET) technique. FRET is a phenomenon in which energy from an excited fluorophore (donor) is non-radiatively transferred to a nearby chromophore (acceptor) if the donor and acceptor are in close proximity (within approximately 10 nm).[97] For example, non-photoconverted and photoconverted Kaede can serve as donor and acceptor, respectively. If Kaede-fused proteins form high-order oligomers, then during photoconversion FRET first increases as green Kaede is

converted to red acceptor and then decreases as the green donor becomes depleted. This methodology was harnessed to confirm that chloroplast 2-cys peroxiredoxin homo-aggregation was dependent on a living plant cell redox state.[98] An orange-to-far red PcFP, PSmOrange2, can be used in combination with green fluorescent proteins such as T-Sapphire for the study of protein-protein interactions.[99] In this case, green fluorescent protein acts as a donor and PSmOrange2 can serve as an acceptor. Because of the fast photoconversion kinetics of PSmOrange2, FRET results in the photoconversion of PSmOrange2. This FRET-facilitated photoswitching was successfully used for monitoring rapamycin-induced dimerization of human FK506-binding protein (FKBP) and FKBP-rapamycin binding domain (FRB); FRET-facilitated photoswitching was also employed for studying interactions between epidermal growth factor (EGF) receptor and Grb2 after stimulation with EGF in HeLa cells.[99] This new mode of FRET-based technique will enhance the study of protein-protein interactions. As photoconversion of PSmOrange2 is irreversible, it will allow tracking of photoconverted protein subsequently to protein-protein interactions, or will allow *in situ* integration of FRET signals derived from transient protein-protein interactions.[99]

In addition to monitoring protein-protein interactions, PtFPs provide an opportunity to manipulate protein-protein interactions by light that can ultimately lead to changes in protein (enzyme) activity and function. While wild type Dronpa is a monomeric PsFP,[8] the Dronpa K145N mutant forms tetramers even at low micromolar concentrations at initial fluorescent state, but redistributes to monomeric dark state upon photoswitching with 500 nm light. Furthermore, it photoswitches back to the original state with 400 nm light with reestablishing tetrameric state. In cultured cells, Dronpa K145N was used to control the protein-protein interactions by fusing it to K-Ras Ct isoprenylation motif (CAAX) and to far-red FP mNeptune. DronpaK145N-CAAX is

targeted to the membrane through isoprenylation. Prior to light manipulation, a subpopulation of mNeptune-DronpaK145N was membrane bound through hetero-oligomerization with DronpaK145N-CAAX. Turning off Dronpa fluorescence resulted in release of mNeptune-DronopaK145N from the membrane due to its monomerization, and turning Dronpa fluorescence back on resulted in binding of mNeptune-DronpaK145N to the membrane again. Thus, reversible photo-manipulation of protein interactions is possible with DronpaK145N. This approach allowed design of enzymes with light-controllable activity by fusing mutants to the enzyme's N- and Ct ends and keeping it in "caged" inactive state prior the light-induced Dronpa dissociation.[100] Thus, as exemplified by Dronpa mutant, PsFPs have potential to become widely applicable optogenetics tools, as the structure of PsFP[9] is well established for further engineering and optimization of novel functions.

In optogenetics, light-regulated ion channels and pumps are frequently used to manipulate the activities of neurons. One challenge of these studies is that, after stimulation of tissues or animals by activating light, it can be difficult to ascertain which specific cells were affected. A solution to this challenge is to co-express a PcFP along with the optogenetics tools such as light-gated ion channels and pumps. For example, in a study seeking correlate inactivation of a subset of neurons in zebrafish with how these specific cells influence behavior, a PcFP was co-expressed along with a plasma membrane ion channel or pump that is activated by light.[101] By focusing an appropriate light source onto a subset of these neurons, the ion channel/pump can be gated while simultaneously photoconverting the PcFP expressed by the cell, thereby labeling the cells irreversibly in red.[101] In this way, these optogenetically manipulated cells can be identified or can be further characterized for their connectivity with other neurons.

Biosensors based on PtFPs

In the past two decades, the number of fluorescence-based and genetically encodable biosensors has expanded dramatically. For example, FP-based sensors take advantage of the fact that GFP can remain fluorescent even after inserting a foreign protein into the GFP. If the inserted protein changes its conformation upon ligand binding while modulating GFP fluorescence, then this fusion protein can be used to indicate specific biological activity or the state of their ambient environment (e.g. local ion concentration) at high spatial and temporal resolution. For example, insertion of calmodulin (CaM), a calcium binding protein, into ECFP, EGFP or EYFP at position Tyr145 resulted in a Ca^{2+}-sensitive fluorescent protein. In EYFP-CaM fusion protein Ca^{2+} binding causes an increase in the 490-nm absorbance peak and a decrease in the 400-nm absorbance peak characteristic for Ca^{2+} free protein.[102] Those initial calcium sensors suffered from low signal-to-noise ratio. Another approach produced calcium sensors by fusing circularly permutated EGFP to CaM and M13 peptide fragment from myosin light chain kinase (a target interactive partner of CaM) at the different ends (N- or Ct). In this sensor, Ca^{2+} binding leads to association of M13/calmodulin and changes in the chromophore environment, increasing the fluorescence intensity 4 - 5 fold.[103] This concept can be also applied to circularly permutated PaFPs and PcFPs, such as EosFP, Kaede, and paGFP, and to generate phototransformable calcium sensor.[104, 105] CaMPARI (calcium-modulated photoactivable ratiometric integrator) is an example of such a circularly permutated [Ca^{2+}] sensor based on green-to-red photoconvertible EosFP, and was applied to entire zebrafish, *Drosophila*, and mouse brain.[105] CaMPARI photoconverts at a much higher rate than EosFP while in the presence

of high [Ca^{2+}] [105], however, cannot photoconvert efficiently under low [Ca^{2+}]. This calcium sensitivity allows labeling of cells that are activated only transiently in response to a stimulus or during short-term behavior. Unlike conventional calcium sensors that are used to monitor [Ca^{2+}] changes in a small population of the cells, CaMPARI can be expressed in a large area of tissue such as mouse brain or freely moving zebrafish larvae and imaged to understand the [Ca^{2+}] changes in the entire neural circuit in response to various environmental stimuli, including odor, light, and vibrations.[105]

Based on PcFPs and PaFPs, fluorescence-based sensors were generated to monitor the autophagy and proteasome-mediated break down of a cell's components. Because photoconversion and photoactivation are irreversible, a decrease in the fluorescence originating from photoactivated and/or photoconverted FPs directly correlates with their degradation rate. Using this principle, fluorescence-based sensors of autophagic activity can be devised by fusing PcFPs to a component of autophagy, enabling fluorescence imaging of the formation and decomposition of autophagic vesicles. By the same principle, fluorescence-based indicators of specific degradation activities can be derived by fusing PcFPs to degron motifs, which are subject to degradation by one of cellular degradation machineries. Macroautophagy is the major mechanism by which the cell breaks down its components, which may include aggregated proteins, lipid membranes, damaged organelles, or other cytoplasmic material. This literal "self-eating" ability of mammalian cells is known to play roles in cell maintenance, energy availability during starvation, differentiation, and disease.[106, 107] The activity of autophagosomes depends on their rates of turnover, which could not be studied by traditional FPs.[108] Thus, sensors for measuring autophagosome life time were designed by fusing Autophagy-related protein 8 (Atg8, also called LC3 in mammals), a protein present on autophagic membranes[109], to a paGFP or

PcFP. For instance, LC3, a mammalian homolog of Atg8, fused to paGFP allowed monitoring lifespan of starvation-induced autophagosomes in normal rat kidney (NRK) cells and demonstrated that the autophagosomes turnover in less than an hour.[110] Another approach was used for quantification of protein turnover by autophagy in tobacco BY-2 cells. In this case the sensor was composed of Cyt b5-KikGR fusion protein that makes aggregates and thus behaves as a substrate for autophagy. Cyt b5-KikGR allows measuring autophagy activity under different starvation conditions.[111]

Sensors were generated to monitor other specific forms of protein degradations, chaperone mediated autophagy (CMA) and proteasome-mediated degradation. CMA is a selective process of protein removal by lysosomes. Substrates of CMA contain KFERQ motif which is recognized by the heat shock cognate protein of 70 kDa (hsc70). Hsc70 delivers the substrates to lysosomes for their degradation.[112] Thus FP fused to the degron motif KFERQ could be a sensor for measuring dynamics of protein association and degradation by lysosomes through CMA. In the past, monitoring of CMA was only possible with *in vitro* assay using isolated lysosomes. As an initial attempt to visualize CMA in living cells, KFERQ was fused to EGFP with an expectation that this fusion would serve as a CMA sensor. However, the lysosome-bound pool of KFERQ-EGFP, because of its low quantity, could not be discriminated from the cytoplasmic pool of KFERQ-EGFP. To overcome this issue of low contrast, KFERQ-motif was fused to photoactivatable or photoconvertible protein. In these cases, only proteins present at photoconversion (or photoactivation) could be highlighted. Because of specific degradation by CMA, the level of cytoplasmic pool decreased overtime, resulting in increased contrast for lysosome-bound pool of KFERQ-PtFPs. Through monitoring the decrease in the level of photoactivated/photoconverted pool, it was possible to determine the rate of KFERQ-

PtFP degradation in living cells without the need for blocking protein synthesis or lysosome/proteasome-mediated degradation. Sensors such as KFERQ-PS-CFP2 and KFERQ-pa(photoactivatable)-mCherry1 were used for measuring basal and induced CMA activity. The study revealed that basal CMA activity is variable among cell types and upregulated under oxidative stress. It also led to the identification of a new crosstalk between CMA and proteasome-mediated proteolysis. Inhibition of proteasome caused increase in basal CMA activity, however had no effect on inducible activity.[113] A CMA sensor was also used in studying CMA activities among different cancer cells. The study demonstrated high basal CMA activities in cancer cells that were necessary for their tumorigenesis. The CMA activity was dependent on the status of macroautophagy in normal cells but not in cancer cells.[114] Likewise CMA- mediated degradation pathway, proteasome-mediated degradation can be effectively studied by PcFP fused to proteins that are well-characterized proteasome substrates. Such proteasome sensors include Dendra2 fused to uncleavable ubiquitin mutant (Ub-G75A/G76V) or ornithine decarboxylase PEST motif.[115] Those different sensors have potential to discriminate ubiquitin dependent (ubiquitin sensor) and independent (PEST sensor) proteasome pathways.

Monitoring protein trafficking and renewal of outer segment in photoreceptor cells

Differential pre-Golgi and post-Golgi sorting of membrane proteins.

The outer segment (OS) is the compartment responsible for light-mediated signaling and is a part of the modified primary cilia in photoreceptor neurons. In rod photoreceptors, GPCR rhodopsin accounts for about 90% of all the membrane proteins in the OS. Unique sorting and

compartmentalization of membrane proteins play critical roles in formation of OS, as well as spatially organizing rhodopsin and the downstream components of the GPCR cascade within the OS. How membrane proteins are sorted, carried by motor-cytoskeletal elements, and accommodated at appropriate membrane domains are still unresolved issues for complicated proteins such as GPCRs. It's been challenging to monitor GPCR transport in real time *in vivo*, because of the lack of technologies to increase contrast for newly synthesized over preexisting proteins. Here, PcFPs provide a unique opportunity to increase contrast for the most recently synthesized proteins. For those purposes, PcFPs which can irreversibly change the emission spectra are suitable, whereas, PaFPs which are not fluorescent prior to conversion are not. After photoconversion of an entire pool of proteins within the cells, fluorescence originating from non-photoconverted PcFPs can be used for monitoring newly synthetized proteins, whereas fluorescence originating from photoconverted PcFPs can be used for monitoring old and preexisting proteins. This concept was proven by using human rhodopsin fused to a green-to-red PcFP Dendra2, and expressed in *Xenopus* rod photoreceptors (Fig. 3A).[116, 117] Within 30 min of photoconversion, newly synthesized proteins, which exhibit green fluorescence, were appreciated in the rod inner segments (ISs) where protein biogenesis occurs (Fig. 3B, left panel, arrow). Some of Rhodopsin-Dendra2 containing vesicles were observed to move vectorially toward the OS. Those moving vesicles transiently shifted from spherical to tubulovesicular shape, indicating that vesicle's shape is influenced by tension due to active trafficking along cytoskeletal element (Fig. 3C, arrows). During our imaging sessions, disk membranes located at the base of the OS incorporated newly synthesized rhodopsin-Dendra2. Thus, active transport of rhodopsin carrier vesicles can be monitored through the use of PcFc (Fig. 3). To the best of our knowledge, this is the first demonstration of GPCR transport from the site of biogenesis to the

final membrane destination. In theory, this technique should be applicable to any membrane proteins fused to PcFPs.

With a technology to visualize transport of membrane protein cargo, previously unanswered questions can be addressed. For example, it is currently unclear how different sorting mechanisms are orchestrated to deliver membrane proteins to the site of OS morphogenesis (see the next section). Within the rod OS, some membrane proteins interact directly while others interact indirectly. Peripherin/rds and cGMP-gated channel are an example of direct interacting partners,[118] and their interaction may play structural role in the OS. Whether this interaction occurs during biogenesis, transport, or after reaching the respective membrane compartments is not entirely clear. On the other hand, rhodopsin and peripherin/rds are considered to be trafficked through different pathways, post-Golgi conventional pathway and unconventional secretory pathway.[119] Either presence or absence of co-trafficking, as well as the interacting site, can be investigated using *in situ* biomolecular fluorescence complementation (BiFC) assay.[120] For this assay, interacting proteins are fused to complementary fragments of fluorescent proteins. When these proteins interact and bring the complementary fragments of a fluorescent protein in close proximity, then the fragments form a functional fluorophore. Thus by analyzing the fluorescence one can visualize the site of interaction within the cells. While previously not attempted, BiFC assay may be combined with PcFPs to clarify the timing of the interaction. In this case, newly formed interactions, instead of newly synthesized proteins, can be labeled by BiFC of PcFPs. Such method would also be useful to visualize co-trafficking of two interacting proteins. The major shortcomings of BiFC, however, are time consuming process of chromophore formation ($T_{1/2} \approx 3000$ s)[121] and irreversibility of protein-protein interactions. Therefore application of BiFC would be limited to the monitoring of stable protein-protein

interactions, and moreover irreversible natures of BiFC would facilitate the detection of artificial interactions enhanced by BiFC itself. In these regards, FRET-facilitated photoswitching would be used in a complementary manner to study relatively transient and reversible protein-protein interactions *in situ*, because FRET-facilitated photoswitching is a very rapid process ($T_{1/2}$ = 50 ~ 100 ms).[99] Transient interactions may occur between small G-proteins and membrane protein cargoes such as rhodopsin, peripherin/rds and cGMP-gated channels in photoreceptor neurons.[122-124] Detection of such interactions would be promoted by FRET-facilitated photoswitching, because concurrent confocal microscopes allow local photoswitching at the selected regions where cargo trafficking occurs (e.g. inner segment in the case of photoreceptor neurons). For both BiFC and FRET-facilitated photoswitching, the expression levels of fusion proteins should be carefully controlled and compared with those of endogenous proteins, because overexpression of fusion proteins will lead to their accumulation and interaction at aberrant cellular locations.

Rod photoreceptor outer segment morphogenesis

The OS requires two separate membrane compartments: disk membranes and OS plasma membrane. Two major models of OS morphogenesis have been proposed. One model is the "endosome model" in which the disk membranes are formed *via* fusion of multiple endosomes into larger disks.[125-127] Another model is the "evagination/rim model". In this model, disk membrane is generated by initial plasma membrane evagination, which then becomes sealed into mature disks as rim and plasma membrane compartments form simultaneously.[128] Both models were based on different EM studies of mouse rod photoreceptors in which evaginations were

either present or absent dependent on chemical fixation or sample preparation methods. As high-resolution electron microscopy is able to capture only the static intermediate process of OS membrane morphogenesis, the methods have been limited to test the hypotheses regarding this dynamic event. Essentially, photoconversion technique allows us to delineate the sequence of events associated with disk morphogenesis. By fusing representatives of each membranous domain to Dendra2 (rhodopsin – disk marker[129]; peripherin/rds – disk rim marker[130] and cGMP gated channel – OS plasma membrane marker[131]), we were able to visualize renewal process of each OS membranous domain under normal and experimentally-manipulated conditions. In normal retina, rhodopsin was added to the evaginations. cGMP gated channel was added to the base of OS lateral plasma membrane, and the process of plasma membrane renewal is synchronized with disk membrane rim formation (Fig. 4A top row). In conjunction with the previous studies, we were able to study the role of F-actin in the sealing of the evagination (Fig. 4A, middle and bottom rows); when F-actin filaments were disrupted experimentally by cytochalasin D, overgrown evaginations were observed as a result of failed sealing of the evaginations.[132, 133] Photoconversion allowed us to discriminate pre-existing evagination which contains old proteins from newly formed evaginations which shall contain only newly formed proteins. Pre-existing and newly formed structure can be discriminated after photoconversion of rhodopsin-Dendra2. After photoconversion and F-actin disruption (Fig. 4A), overgrown evaginations contained both green and red rhodopsin-Dendra2 (Fig. 4A, middle and bottom rows, arrows). Thus, the overgrowths were not formed *de novo*, but formed from the preexisted evaginations. In addition, failure of disk sealing upon F-actin disorganization is apparent from aberrant trafficking of disk rim and OS plasma membrane components, peripherin/rds and cGMP-gated channels. Aberrant subciliary trafficking of cGMP gated channel was evidenced by

accumulation of newly synthesized CNGA1-Dendra2 at the basal OS PM (Fig. 4A, bottom row, asterisks), and aberrant trafficking of peripherin/rds (Fig. 4A, bottom row, arrow heads) was evidenced by peripherin/rds-Dendra2's failure to enter the mature disk rim region.

While the study so far delineates the process of OS morphogenesis, the detailed molecular mechanism of disk sealing (rim formation) is still unclear. Prior to rim formation, evaginations contain prominin-1 and photoreceptor-specific cadherin (PCDH21).[134-137] During rim formation, it is likely that those two proteins are displaced by peripherin/rds (Fig. 4B). In addition to displacement, the PCDH21 undergoes proteolytic cleavage[138] which may be associated with the disk closure event. Thus, membrane morphogenesis and trafficking of multiple membrane proteins are highly coordinated and synchronized events. Therefore, to fully understand disk membrane morphogenesis it is desirable to visualize the relative timing of membrane protein incorporation or displacement by simultaneous imaging of two or more components. We envision that such co-visualization would be possible since PcFPs with distinct emission/excitation spectra (e.g. combination of PS-CFP2[70] and PSmOrange[5]) are becoming available to discriminate new and old pools of two distinct protein populations (e.g. peripherin/rds and prominin-1).

In addition to the above mentioned advance in visualizing multiple components, improving the imaging resolution for visualizing individual disk morphogenic event is the next step to refine our understanding of OS membrane morphogenesis (Fig. 4B). Disk membranes are separated by interdiskal cytoplasmic space at a distance of ~ 15 nm. Thus with the thickness of disk at ~ 5 nm, single disk or evagination is observed every ~ 20 nm.[128, 139] Conventional light-microscopy can only resolve structures separated longer than ~ 200 nm distance, and thus has limited capability to resolve the structures associated with disk morphogenesis. For example, any

resolution improvement surpassing diffraction limit would facilitate the analysis of gradual growth in evagination structures which was not possible with conventional light microscopy. Recent developments of new PtFPs contributed to the high-resolution imaging techniques that could possibly resolve this issue. RsFP such as rsEGFP is essential for the imaging technique called RESOLFT. RESOLFT is similar to STED microscopy in terms of the mechanism, but requires much less light energy to accomplish sub-diffraction resolution, and thus suitable for live imaging.[140, 141] RsFP Dronpa and its variants have been successfully used in live imaging by a technique called photochromic stochastic optical fluctuation imaging (pcSOFI).[142] This technique allows two- to threefold improved spatial resolution over the resolution attainable by conventional optical microscopy.[143] Although the improvement is not as high as in techniques such as photoactivated localization microscopy (PALM), pcSOFI is more suited than PALM for live imaging. pcSOFI and RESOLFT can accomplish ~50 nm resolution, and likely useful to visualize gradual growths of evaginations in *Xenopus laevis* rod photoreceptors. In addition, pcSOFI offers better temporal resolution, does not require specialized equipment, and can produce superresolution images over different range of imaging conditions. Recently, a green-to-red photoconvertible Dronpa mutant was engineered (pcDronpa2) that is compatible with pcSOFI microscopy and PALM,[144] accomplishing the superresolution imaging for both non-photoconverted (green) and photoconverted (red) isoforms of pcDronpa2. A Dendra2 mutant NijiFP combines photoconvertible and biphotochromic properties, and thus would be compatible with PALM[10] which can accomplish ~20 nm imaging resolution. Therefore, these new PcFPs with unique photochromic natures will, in theory, allow obtaining high resolution images for newly forming disks.

Fate of mislocalized rhodopsin.

While rhodopsin is localized to the OS under normal conditions, it mislocalizes to IS plasma membrane as well as somatic and synaptic plasma membrane under many different pathological conditions including retinitis pigmentosa (RP). While these genetic and other pathological conditions can lead to the mislocalization, defects in the trafficking signal located at rhodopsin Ct tail cause some of the most severe forms of RP.[124] For example, a naturally occurring mutation in rhodopsin that causes loss of last five amino acids at Ct tail, Q344ter, mislocalizes in the rod photoreceptors.[145] Other than rhodopsin mutations, defects in trafficking machineries, such as molecular motors[146] or small guanine nucleotide-binding proteins,[147] can cause rhodopsin mislocalization and associated diseases. At the plasma membrane, mislocalized rhodopsin likely activates aberrant signaling pathways that are proapoptotic. This toxicity is dependent on the amount of mislocalized rhodopsin[146, 148] which makes it critical to analyze how the mislocalized rhodopsin is regulated. The amount of any membrane proteins would be regulated by the balance between new synthesis, delivery of new protein to the membrane, and removal of protein from the membrane. PcFPs are highly suited for monitoring each of these steps.

To test the hypothesis that the level of plasma membrane mislocalized rhodopsin is renewed, we took advantage of rhodopsin Q344ter mutant fused to Dendra2 (RhoQ344ter-Dendra2). This allowed us to discriminate old rhodopsin Q344ter preexisting in the plasma membrane and newly synthesized rhodopsin Q344ter that are trafficked to the plasma membrane. After several days post-photoconversion, we noticed that the compartments of the photoreceptor that exhibited the most mislocalization (IS plasma membrane and calyceal processes) had slowly changed from red, to yellow, and lastly to green, indicating a renewal of protein to those regions

(Fig. 5A, arrows).[116] Then this observation suggested that red Q344ter was removed and eliminated form rod cells. In the previous studies with mouse models of rhodopsin mislocalization,[149, 150] numerous rhodopsin baring vesicles were observed in the interphotoreceptor matrix. In *Xenopus* model expressing mislocalization prone RhoQ344ter-Dendra2, similar extracellular vesicles were observed to contain RhoQ344ter-Dendra2 (Fig. 5A, arrowheads), indicating that mislocalized proteins are removed through vesicle release.[116] Photoconversion technique was instructive to the source of vesicles as well. The color of extracellular vesicles showed gradual shift of color from green to yellow and to red (Fig. 5B).[116] This transition of old to new protein coincides with the color shift of the plasma membrane, suggesting that the protein originated from mislocalized rhodopsin on the plasma membrane. In addition to vesicle release, lysosome may also mediate the degradation of RhoQ344ter (Fig. 5B). In rod cells expressing RhoQ344ter-Dendra2, lysosome membrane protein, LAPM1, was highly upregulated,[116] suggesting that lysosome-mediated pathway is affected by rhodopsin mislocalization. In this regard, specific labeling of lysosome or autophagosome structures using far-red fluorescent proteins,[151] along with RhoQ344ter-Dendra2, will facilitate the study of lysosome-mediated degradation (Fig. 5B). For example, labeling of lysosomes and autophagosomes were previously accomplished with LAMP1[152] and LC3[110, 153] fused to fluorescent proteins, respectively. In addition to the Q344ter mutant, rhodopsin mislocalization can be caused by its aberrant arrestin binding such as in constitutively active rhodopsin mutants (K296E and K296M) or light-independently hyperphosphorylated rhodopsin mutants (R135A and R135L).[124] In general, arrestin binding causes targeting of GPCRs to the endolysosomal system, and other rhodopsin mutants may also depend on lysosome for their degradation.[124] Thus

the approach taken for RhoQ344ter could be applied to study the transport and degradation of rhodopsin mutants whose mislocalization depends on aberrant arrestin binding.

Acknowledgements

This work was supported by the U.S. National Institutes of Health grants EY020826, EY011373, and EY007157.

Table 1. Properties of PtFPs for which applications were mentioned in this manuscript

Protein	λ_{max} ((ex/em (nm))[a]		ε ($mM^{-1}cm^{-1}$)[a]		Φ_{fluo}[a]		Actinic light[b] (nm)	Application
	PRE	POST	PRE	POST	PRE	POST		
Photoconvertible fluorescent protein (PcFPs)								
Kaede[1]	508/518	572/580	98.8	60.4	0.88	0.33	405	Cell migration during embryogenesis, tissue regeneration and immune response[17-19, 24, 26, 29, 30, 32]; Determining birthdates of cells[28]; Dynamic processes associated with Golgi[53, 54] and centrosome[55, 56, 154]; Protein endocytosis[78] and homo-oligomerization[98]; Ca^{2+} sensors[104]
KikGR[64]	507/517	583/593	53.7	35.1	0.70	0.65	405	Cell migration during embryogenesis in different animal models[20-22]; Autophagy activity sensor in plants[111]
mKikGR[64]	505/515	580/591	49.0	28.0	0.69	0.63	405	Pathogen/host interaction[33]
EosFP[61]	506/516	571/581	72.0	41.0	0.7	0.55	405	Monitoring the division and lineage of vertebrate embryonic cells[23]; single particle tracking[95]; Ca^{2+} sensor[104, 105]
mEosFP[61]	505/516	569/581	67.2	37.0	0.64	0.62	405	Plastids dynamics[50]
mEos2[46]	506/519	573/584	56.0	46.0	0.84	0.66	405	Tracking peroxisomes[47]; Monitoring protein dynamics in cilia[59]
Dendra2[70]	490/553	507/573	45.0	35.0	0.50	0.55	405/ 488	Cell movement during fin regeneration in zebrafish[25]; Mitochondria dynamics[45]; Tracking individual insulin granules[82]; Measuring proteasome activity[115]; Monitoring protein (mis)trafficking in rod photoreceptor cells and ROS[a] morphogenesis[116, 133, 155, 119]
PSmOrange2[99]	546/561	619/651	51.0	18.9	0.61	0.38	488	Protein-protein interactions in combination with green FP[a] (FRET[a]-facilitated photoswitching) [99]
PS-CFP2[70]	400/468	490/511	43.0	47.0	0.20	0.23	405	CMA[a] sensor[113]
Photoactivable fluorescent proteins (PaFPs)								
paGFP[2]	400/515	504/517	20.7	17.4	0.13	0.79	405	Monitoring mesoderm migration in the early embryonic development of *Drosophila melanogaster*[27]; Mitochondria,[34-40] lysosome,[2] Golgi[52] and protein[84-86, 87, 88, 90] dynamics; Tracking individual insulin granules[82]; Ca^{2+} sensors[104]; Autophagy activity

								sensors[110]
pa-mCherry1[6]	(404)/ND[a]	565/595	6.5	18.0	ND[a]	0.46	405	CMA[a] sensor[114]
paTagRFP[96]	-	564/595	-	66.0	-	0.38	405	Two-color single-particle tracking[96]
Photoswitchable fluorescent proteins (PsFPs)								
Dronpa[8]	(392)/ND[a]	503/518	ND[a]	95.0	ND[a]	0.85	405/ 488	Manipulating protein-protein interactions by light[100]; Monitoring protein exchange among different cellular compartments[8] and comparing viscosity of different cytoplasmic compartments[89]

[a]abbreviations: λ_{max} ex/em: maximum of excitation/emission spectrum; ε: molar extinction coefficient; Φ_{fluo}: fluorescence quantum yield; ROS: rod outer segment; FP: fluorescent protein; FRET: Förster resonance energy transfer; CMA: chaperone mediated autophagy; ND: not determined;

[b]Light wavelengths needed for the phototransformation.

Figure legends

Figure 1. Light-induced chromophore transformations in phototransformable fluorescence proteins (PtFPs). Examples of irreversibly photoconvertible fluorescent proteins (EosFP and PSmOrange) (A,B), photoactivatable green fluorescent protein (paGFP) (C), and photoswitchable fluorescence protein (Dronpa) (D). Ox, oxidant molecule; OxH, reduced oxidant molecule; *hv,* irradiation with light.

Figure 2. Application of PtFPs in visualizing biological processes. (A) Tracking of cell movement and differentiation, determination of cells' birthdates, and monitoring of metabolism in pathogens. After photoconversion/photoactivation, individual cells can be distinguished from their surrounding and monitored over time. (B) PaFPs and PcFPs were used to study mitochondria interactions (1); Golgi dynamics and secretory pathway (2); inheritance pattern of centrioles (3) and exchange of signaling components in cilia (4). (C) Models of monitoring protein diffusion by fluorescence decay after photoactivation (FDAP), monitoring membrane protein endocytosis, and tracking single particle. (D) Visualization of protein translocation by PsFPs.

Figure 3. Application of the PcFP Dendra2 for imaging of rhodopsin trafficking in live *Xenopus laevis* rod photoreceptor cells. (A) Schematic representation of the photoconversion (PC) technique. Rhodopsin fused to Dendra2 (rhodopsin-Dendra2) is green prior to PC, and is switched to red after PC. New rhodopsin-Dendra2 (green) is synthetized in the inner segment and trafficked to the outer segment where it gets incorporated into disks. (B, C) Live *Xenopus laevis* rod photoreceptor cells expressing rhodopsin-Dendra2. Newly synthetized rhodopsin-Dendra2 can be observed in the inner segment shortly after PC (B, left panel, arrow); Rod outer

segments are renewed over days (B, middle and right panel). (C) Vesicles containing newly synthetized rhodopsin-Dendra2 can be seen moving from the inner toward the outer segment. Images are maximum projections of optical slices. Scale bars, 10 μm. Images in (B) and (C) were adopted from Lodowski *et al.*[116]

Figure 4. Application of PcFP Dendra2 for monitoring photoreceptor outer segment morphogenesis. Under normal conditions newly synthetized (green) rhodopsin-Dendra2 is incorporated into the evaginations, peripherin/rds-Dendra2 into the disk rim region, and cGMP gated channel (CNGA1-Dendra2) into the plasma membrane (A, upper row). When F-actin is disrupted, disks fail to mature and precursors of disks (evaginations) overgrow (A, middle and bottom row). Overgrown evaginations contain preexisting (red) and newly added rhodopsin-Dendra2 (green) (A, middle and bottom rows, arrows) and only newly synthetized peripherin/rds-Dendra2 (A, middle and bottom rows, arrow heads). In the absence of disk formation, CNGA1-Dendra2 cannot enter the outer segment (A, middle row, asterisk). Images are maximum projections of optical slices. The top panel of CNGA1 was adapted from Nemet *et al.*[133] Scale bars, 10 μm. (B) A model describing rod disk membrane morphogenesis. In this model, evaginations grow gradually at the base of the outer segment. The growth accompanies with accommodation of PCDH21 and prominin-1 which facilitate the formation of membrane protrusion. After complete growth of evagination, rim region of disk is formed, leading to accommodation of peripherin/rds, expulsion of prominin-1 and proteolysis of PCDH21. Rim formation coincides with sealing of evagination and separation of disk from the plasma membrane.

Figure 5. Monitoring removal of mislocalized mutant rhodopsin (Q344ter) in live *Xenopus laevis* rod photoreceptor cells. (A) RhodopsinQ344ter-Dendra2 mislocalizes to the inner segment

plasma membrane including calyceal processes (arrows). Over time mislocalized rhodopsin is renewed at the plasma membrane (arrows). At 2 days post photoconversion (2 d post-PC), the plasma membrane is yellow because it is occupied with both old (red) and new (green) RhodopsinQ344ter-Dendra2. At 6 days post photoconversion (6 d post-PC), old RhodopsinQ344ter-Dendra2 was removed and new RhodopsinQ344ter-Dendra2 was added, resulting in green fluorescent plasma membrane. Images are maximum projections of confocal sections, and were adopted from Lodowski *et al.*[116] Scale bar, 10 μm. (B) Schematic representations of hypothetical mechanisms involved in removal of mislocalized rhodopsin, and how a green-to-red PcFP can be used unravel those mechanisms. MVB stands for multivesicular body.

References

1. R. Ando, H. Hama, M. Yamamoto-Hino, H. Mizuno and A. Miyawaki, *An optical marker based on the UV-induced green-to-red photoconversion of a fluorescent protein, Proc Natl Acad Sci U S A*, 2002, **99**, 12651-12656.
2. G. H. Patterson and J. Lippincott-Schwartz, *A photoactivatable GFP for selective photolabeling of proteins and cells, Science*, 2002, **297**, 1873-1877.
3. K. Nienhaus, G. U. Nienhaus, J. Wiedenmann and H. Nar, *Structural basis for photo-induced protein cleavage and green-to-red conversion of fluorescent protein EosFP, Proc Natl Acad Sci U S A*, 2005, **102**, 9156-9159.
4. V. Adam, K. Nienhaus, D. Bourgeois and G. U. Nienhaus, *Structural basis of enhanced photoconversion yield in green fluorescent protein-like protein Dendra2, Biochemistry*, 2009, **48**, 4905-4915.
5. O. M. Subach, G. H. Patterson, L. M. Ting, Y. Wang, J. S. Condeelis and V. V. Verkhusha, *A photoswitchable orange-to-far-red fluorescent protein, PSmOrange, Nat Methods*, 2011, **8**, 771-777.
6. F. V. Subach, V. N. Malashkevich, W. D. Zencheck, H. Xiao, G. S. Filonov, S. C. Almo and V. V. Verkhusha, *Photoactivation mechanism of PAmCherry based on crystal structures of the protein in the dark and fluorescent states, Proc Natl Acad Sci U S A*, 2009, **106**, 21097-21102.
7. J. J. van Thor, T. Gensch, K. J. Hellingwerf and L. N. Johnson, *Phototransformation of green fluorescent protein with UV and visible light leads to decarboxylation of glutamate 222, Nat Struct Biol*, 2002, **9**, 37-41.

8. R. Ando, H. Mizuno and A. Miyawaki, *Regulated fast nucleocytoplasmic shuttling observed by reversible protein highlighting, Science*, 2004, **306**, 1370-1373.
9. M. Andresen, A. C. Stiel, S. Trowitzsch, G. Weber, C. Eggeling, M. C. Wahl, S. W. Hell and S. Jakobs, *Structural basis for reversible photoswitching in Dronpa, Proc Natl Acad Sci U S A*, 2007, **104**, 13005-13009.
10. V. Adam, B. Moeyaert, C. C. David, H. Mizuno, M. Lelimousin, P. Dedecker, R. Ando, A. Miyawaki, J. Michiels, Y. Engelborghs and J. Hofkens, *Rational design of photoconvertible and biphotochromic fluorescent proteins for advanced microscopy applications, Chem Biol*, 2011, **18**, 1241-1251.
11. J. Fuchs, S. Bohme, F. Oswald, P. N. Hedde, M. Krause, J. Wiedenmann and G. U. Nienhaus, *A photoactivatable marker protein for pulse-chase imaging with superresolution, Nat Methods*, 2010, **7**, 627-630.
12. V. Adam, *Phototransformable fluorescent proteins: which one for which application?, Histochem Cell Biol*, 2014, **142**, 19-41.
13. V. Adam, R. Berardozzi, M. Byrdin and D. Bourgeois, *Phototransformable fluorescent proteins: Future challenges, Curr Opin Chem Biol*, 2014, **20**, 92-102.
14. C. Duan, V. Adam, M. Byrdin and D. Bourgeois, *Structural basis of photoswitching in fluorescent proteins, Methods Mol Biol*, 2014, **1148**, 177-202.
15. R. W. Young, *The renewal of photoreceptor cell outer segments, The Journal of cell biology*, 1967, **33**, 61-72.
16. D. S. Williams, *Photoreceptor cell biology and inherited retinal degenerations*, World Scientific, 2004.
17. K. Hatta, H. Tsujii and T. Omura, *Cell tracking using a photoconvertible fluorescent protein, Nat Protoc*, 2006, **1**, 960-967.
18. T. Sato, M. Takahoko and H. Okamoto, *HuC:Kaede, a useful tool to label neural morphologies in networks in vivo, Genesis*, 2006, **44**, 136-142.
19. T. Mutoh, T. Miyata, S. Kashiwagi, A. Miyawaki and M. Ogawa, *Dynamic behavior of individual cells in developing organotypic brain slices revealed by the photoconvertable protein Kaede, Exp Neurol*, 2006, **200**, 430-437.
20. P. M. Kulesa, J. M. Teddy, D. A. Stark, S. E. Smith and R. McLennan, *Neural crest invasion is a spatially-ordered progression into the head with higher cell proliferation at the migratory front as revealed by the photoactivatable protein, KikGR, Dev Biol*, 2008, **316**, 275-287.
21. D. A. Stark and P. M. Kulesa, *An in vivo comparison of photoactivatable fluorescent proteins in an avian embryo model, Dev Dyn*, 2007, **236**, 1583-1594.
22. S. Nowotschin and A. K. Hadjantonakis, *Use of KikGR a photoconvertible green-to-red fluorescent protein for cell labeling and lineage analysis in ES cells and mouse embryos, BMC Dev Biol*, 2009, **9**, 49.
23. S. A. Wacker, F. Oswald, J. Wiedenmann and W. Knochel, *A green to red photoconvertible protein as an analyzing tool for early vertebrate development, Dev Dyn*, 2007, **236**, 473-480.
24. K. Geurtzen, F. Knopf, D. Wehner, L. F. Huitema, S. Schulte-Merker and G. Weidinger, *Mature osteoblasts dedifferentiate in response to traumatic bone injury in the zebrafish fin and skull, Development*, 2014, **141**, 2225-2234.
25. W. P. Dempsey, S. E. Fraser and P. Pantazis, *PhOTO zebrafish: a transgenic resource for in vivo lineage tracing during development and regeneration, PLoS One*, 2012, **7**, e32888.
26. K. Kishi, T. A. Onuma and H. Nishida, *Long-distance cell migration during larval development in the appendicularian, Oikopleura dioica, Dev Biol*, 2014, **395**, 299-306.
27. M. J. Murray and R. Saint, *Photoactivatable GFP resolves Drosophila mesoderm migration behaviour, Development*, 2007, **134**, 3975-3983.

28. S. J. Caron, D. Prober, M. Choy and A. F. Schier, *In vivo birthdating by BAPTISM reveals that trigeminal sensory neuron diversity depends on early neurogenesis, Development*, 2008, **135**, 3259-3269.
29. M. Tomura, N. Yoshida, J. Tanaka, S. Karasawa, Y. Miwa, A. Miyawaki and O. Kanagawa, *Monitoring cellular movement in vivo with photoconvertible fluorescence protein "Kaede" transgenic mice, Proc Natl Acad Sci U S A*, 2008, **105**, 10871-10876.
30. M. Tomura, T. Honda, H. Tanizaki, A. Otsuka, G. Egawa, Y. Tokura, H. Waldmann, S. Hori, J. G. Cyster, T. Watanabe, Y. Miyachi, O. Kanagawa and K. Kabashima, *Activated regulatory T cells are the major T cell type emigrating from the skin during a cutaneous immune response in mice, J Clin Invest*, 2010, **120**, 883-893.
31. Y. Imanishi, K. H. Lodowski and Y. Koutalos, *Two-photon microscopy: shedding light on the chemistry of vision, Biochemistry*, 2007, **46**, 9674-9684.
32. T. Chtanova, H. R. Hampton, L. A. Waterhouse, K. Wood, M. Tomura, Y. Miwa, C. R. Mackay, R. Brink and T. G. Phan, *Real-time interactive two-photon photoconversion of recirculating lymphocytes for discontinuous cell tracking in live adult mice, J Biophotonics*, 2014, **7**, 425-433.
33. A. J. Muller, S. Aeschlimann, R. Olekhnovitch, M. Dacher, G. F. Spath and P. Bousso, *Photoconvertible pathogen labeling reveals nitric oxide control of Leishmania major infection in vivo via dampening of parasite metabolism, Cell Host Microbe*, 2013, **14**, 460-467.
34. A. Lovy, A. J. Molina, F. M. Cerqueira, K. Trudeau and O. S. Shirihai, *A faster, high resolution, mtPA-GFP-based mitochondrial fusion assay acquiring kinetic data of multiple cells in parallel using confocal microscopy, Journal of visualized experiments : JoVE*, 2012, e3991.
35. M. Karbowski, D. Arnoult, H. Chen, D. C. Chan, C. L. Smith and R. J. Youle, *Quantitation of mitochondrial dynamics by photolabeling of individual organelles shows that mitochondrial fusion is blocked during the Bax activation phase of apoptosis, The Journal of cell biology*, 2004, **164**, 493-499.
36. M. Karbowski, M. M. Cleland and B. A. Roelofs, *Photoactivatable green fluorescent protein-based visualization and quantification of mitochondrial fusion and mitochondrial network complexity in living cells, Methods in enzymology*, 2014, **547**, 57-73.
37. S. B. Berman, Y. B. Chen, B. Qi, J. M. McCaffery, E. B. Rucker, 3rd, S. Goebbels, K. A. Nave, B. A. Arnold, E. A. Jonas, F. J. Pineda and J. M. Hardwick, *Bcl-x L increases mitochondrial fission, fusion, and biomass in neurons, The Journal of cell biology*, 2009, **184**, 707-719.
38. R. Anand, T. Wai, M. J. Baker, N. Kladt, A. C. Schauss, E. Rugarli and T. Langer, *The i-AAA protease YME1L and OMA1 cleave OPA1 to balance mitochondrial fusion and fission, The Journal of cell biology*, 2014, **204**, 919-929.
39. Y. J. Lee, S. Y. Jeong, M. Karbowski, C. L. Smith and R. J. Youle, *Roles of the mammalian mitochondrial fission and fusion mediators Fis1, Drp1, and Opa1 in apoptosis, Molecular biology of the cell*, 2004, **15**, 5001-5011.
40. X. Huang, L. Sun, S. Ji, T. Zhao, W. Zhang, J. Xu, J. Zhang, Y. Wang, X. Wang, C. Franzini-Armstrong, M. Zheng and H. Cheng, *Kissing and nanotunneling mediate intermitochondrial communication in the heart, Proc Natl Acad Sci U S A*, 2013, **110**, 2846-2851.
41. F. Legros, A. Lombes, P. Frachon and M. Rojo, *Mitochondrial fusion in human cells is efficient, requires the inner membrane potential, and is mediated by mitofusins, Molecular biology of the cell*, 2002, **13**, 4343-4354.
42. N. Ishihara, A. Jofuku, Y. Eura and K. Mihara, *Regulation of mitochondrial morphology by membrane potential, and DRP1-dependent division and FZO1-dependent fusion reaction in mammalian cells, Biochemical and biophysical research communications*, 2003, **301**, 891-898.

43. H. Chen, S. A. Detmer, A. J. Ewald, E. E. Griffin, S. E. Fraser and D. C. Chan, *Mitofusins Mfn1 and Mfn2 coordinately regulate mitochondrial fusion and are essential for embryonic development, The Journal of cell biology*, 2003, **160**, 189-200.
44. Y. Mattenberger, D. I. James and J. C. Martinou, *Fusion of mitochondria in mammalian cells is dependent on the mitochondrial inner membrane potential and independent of microtubules or actin, FEBS letters*, 2003, **538**, 53-59.
45. A. H. Pham, J. M. McCaffery and D. C. Chan, *Mouse lines with photo-activatable mitochondria to study mitochondrial dynamics, Genesis*, 2012, **50**, 833-843.
46. S. A. McKinney, C. S. Murphy, K. L. Hazelwood, M. W. Davidson and L. L. Looger, *A bright and photostable photoconvertible fluorescent protein, Nat Methods*, 2009, **6**, 131-133.
47. S. Richert, S. Kleinecke, J. Gunther, F. Schaumburg, J. Edgar, G. U. Nienhaus, K. A. Nave and C. M. Kassmann, *In vivo labeling of peroxisomes by photoconvertible mEos2 in myelinating glia of mice, Biochimie*, 2014, **98**, 127-134.
48. R. H. Kohler, J. Cao, W. R. Zipfel, W. W. Webb and M. R. Hanson, *Exchange of protein molecules through connections between higher plant plastids, Science*, 1997, **276**, 2039-2042.
49. E. Y. Kwok and M. R. Hanson, *GFP-labelled Rubisco and aspartate aminotransferase are present in plastid stromules and traffic between plastids, J Exp Bot*, 2004, **55**, 595-604.
50. M. H. Schattat, S. Griffiths, N. Mathur, K. Barton, M. R. Wozny, N. Dunn, J. S. Greenwood and J. Mathur, *Differential coloring reveals that plastids do not form networks for exchanging macromolecules, Plant Cell*, 2012, **24**, 1465-1477.
51. M. H. Schattat, K. A. Barton and J. Mathur, *The myth of interconnected plastids and related phenomena, Protoplasma*, 2015, **252**, 359-371.
52. J. H. Tam, C. Seah and S. H. Pasternak, *The Amyloid Precursor Protein is rapidly transported from the Golgi apparatus to the lysosome and where it is processed into beta-amyloid, Molecular brain*, 2014, **7**, 54.
53. S. C. Brown, S. Bolte, M. Gaudin, C. Pereira, J. Marion, M. N. Soler and B. Satiat-Jeunemaitre, *Exploring plant endomembrane dynamics using the photoconvertible protein Kaede, Plant J*, 2010, **63**, 696-711.
54. M. Bourge, C. Fort, M. N. Soler, B. Satiat-Jeunemaitre and S. C. Brown, *A pulse-chase strategy combining click-EdU and photoconvertible fluorescent reporter: tracking Golgi protein dynamics during the cell cycle, New Phytol*, 2015, **205**, 938-950.
55. J. Januschke, S. Llamazares, J. Reina and C. Gonzalez, *Drosophila neuroblasts retain the daughter centrosome, Nature communications*, 2011, **2**, 243.
56. J. H. Imai, X. Wang and S. H. Shi, *Kaede-centrin1 labeling of mother and daughter centrosomes in mammalian neocortical neural progenitors, Curr Protoc Stem Cell Biol*, 2010, **Chapter 5**, Unit 5A 5.
57. X. Wang, J. W. Tsai, J. H. Imai, W. N. Lian, R. B. Vallee and S. H. Shi, *Asymmetric centrosome inheritance maintains neural progenitors in the neocortex, Nature*, 2009, **461**, 947-955.
58. S. Mukhopadhyay and R. Rohatgi, *G-protein-coupled receptors, Hedgehog signaling and primary cilia, Seminars in cell & developmental biology*, 2014, **33**, 63-72.
59. J. Kim, E. Y. Hsia, J. Kim, N. Sever, P. A. Beachy and X. Zheng, *Simultaneous measurement of smoothened entry into and exit from the primary cilium, PLoS One*, 2014, **9**, e104070.
60. R. M. Wachter, J. L. Watkins and H. Kim, *Mechanistic diversity of red fluorescence acquisition by GFP-like proteins, Biochemistry*, 2010, **49**, 7417-7427.
61. J. Wiedenmann, S. Ivanchenko, F. Oswald, F. Schmitt, C. Rocker, A. Salih, K. D. Spindler and G. U. Nienhaus, *EosFP, a fluorescent marker protein with UV-inducible green-to-red fluorescence conversion, Proc Natl Acad Sci U S A*, 2004, **101**, 15905-15910.

62. J. Mathur, R. Radhamony, A. M. Sinclair, A. Donoso, N. Dunn, E. Roach, D. Radford, P. S. Mohaghegh, D. C. Logan, K. Kokolic and N. Mathur, *mEosFP-based green-to-red photoconvertible subcellular probes for plants, Plant Physiol*, 2010, **154**, 1573-1587.
63. N. G. Gurskaya, V. V. Verkhusha, A. S. Shcheglov, D. B. Staroverov, T. V. Chepurnykh, A. F. Fradkov, S. Lukyanov and K. A. Lukyanov, *Engineering of a monomeric green-to-red photoactivatable fluorescent protein induced by blue light, Nat Biotechnol*, 2006, **24**, 461-465.
64. S. Habuchi, H. Tsutsui, A. B. Kochaniak, A. Miyawaki and A. M. van Oijen, *mKikGR, a monomeric photoswitchable fluorescent protein, PloS one*, 2008, **3**, e3944.
65. H. Tsutsui, S. Karasawa, H. Shimizu, N. Nukina and A. Miyawaki, *Semi-rational engineering of a coral fluorescent protein into an efficient highlighter, EMBO reports*, 2005, **6**, 233-238.
66. D. A. Zacharias, J. D. Violin, A. C. Newton and R. Y. Tsien, *Partitioning of lipid-modified monomeric GFPs into membrane microdomains of live cells, Science*, 2002, **296**, 913-916.
67. M. Zhang, H. Chang, Y. Zhang, J. Yu, L. Wu, W. Ji, J. Chen, B. Liu, J. Lu, Y. Liu, J. Zhang, P. Xu and T. Xu, *Rational design of true monomeric and bright photoactivatable fluorescent proteins, Nat Methods*, 2012, **9**, 727-729.
68. H. Hoi, N. C. Shaner, M. W. Davidson, C. W. Cairo, J. Wang and R. E. Campbell, *A monomeric photoconvertible fluorescent protein for imaging of dynamic protein localization, Journal of molecular biology*, 2010, **401**, 776-791.
69. D. M. Chudakov, S. Lukyanov and K. A. Lukyanov, *Using photoactivatable fluorescent protein Dendra2 to track protein movement, Biotechniques*, 2007, **42**, 553, 555, 557 passim.
70. D. M. Chudakov, S. Lukyanov and K. A. Lukyanov, *Tracking intracellular protein movements using photoswitchable fluorescent proteins PS-CFP2 and Dendra2, Nat Protoc*, 2007, **2**, 2024-2032.
71. K. Nienhaus and G. U. Nienhaus, *Fluorescent proteins for live-cell imaging with super-resolution, Chemical Society reviews*, 2014, **43**, 1088-1106.
72. N. C. Shaner, M. Z. Lin, M. R. McKeown, P. A. Steinbach, K. L. Hazelwood, M. W. Davidson and R. Y. Tsien, *Improving the photostability of bright monomeric orange and red fluorescent proteins, Nat Methods*, 2008, **5**, 545-551.
73. S. Kuruppu, N. Tochon-Danguy and A. I. Smith, *Applicability of green fluorescence protein in the study of endothelin converting enzyme-1c trafficking, Protein science : a publication of the Protein Society*, 2013, **22**, 306-313.
74. Shemiakina, II, G. V. Ermakova, P. J. Cranfill, M. A. Baird, R. A. Evans, E. A. Souslova, D. B. Staroverov, A. Y. Gorokhovatsky, E. V. Putintseva, T. V. Gorodnicheva, T. V. Chepurnykh, L. Strukova, S. Lukyanov, A. G. Zaraisky, M. W. Davidson, D. M. Chudakov and D. Shcherbo, *A monomeric red fluorescent protein with low cytotoxicity, Nature communications*, 2012, **3**, 1204.
75. V. Magidson and A. Khodjakov, *Circumventing photodamage in live-cell microscopy, Methods in cell biology*, 2013, **114**, 545-560.
76. N. C. Shaner, P. A. Steinbach and R. Y. Tsien, *A guide to choosing fluorescent proteins, Nat Methods*, 2005, **2**, 905-909.
77. S. Brogi, A. Tafi, L. Desaubry and C. G. Nebigil, *Discovery of GPCR ligands for probing signal transduction pathways, Frontiers in pharmacology*, 2014, **5**, 255.
78. A. Schmidt, B. Wiesner, K. Weisshart, K. Schulz, J. Furkert, B. Lamprecht, W. Rosenthal and R. Schulein, *Use of Kaede fusions to visualize recycling of G protein-coupled receptors, Traffic*, 2009, **10**, 2-15.
79. A. Varadi, E. K. Ainscow, V. J. Allan and G. A. Rutter, *Involvement of conventional kinesin in glucose-stimulated secretory granule movements and exocytosis in clonal pancreatic beta-cells, Journal of cell science*, 2002, **115**, 4177-4189.

80. M. Ohara-Imaizumi, Y. Nakamichi, T. Tanaka, H. Ishida and S. Nagamatsu, *Imaging exocytosis of single insulin secretory granules with evanescent wave microscopy: distinct behavior of granule motion in biphasic insulin release, J Biol Chem*, 2002, **277**, 3805-3808.
81. M. Hao, X. Li, M. A. Rizzo, J. V. Rocheleau, B. M. Dawant and D. W. Piston, *Regulation of two insulin granule populations within the reserve pool by distinct calcium sources, Journal of cell science*, 2005, **118**, 5873-5884.
82. S. Baltrusch and S. Lenzen, *Monitoring of glucose-regulated single insulin secretory granule movement by selective photoactivation, Diabetologia*, 2008, **51**, 989-996.
83. A. Miyawaki, *Proteins on the move: insights gained from fluorescent protein technologies, Nat Rev Mol Cell Biol*, 2011, **12**, 656-668.
84. G. Kaur, M. W. Costa, C. M. Nefzger, J. Silva, J. C. Fierro-Gonzalez, J. M. Polo, T. D. Bell and N. Plachta, *Probing transcription factor diffusion dynamics in the living mammalian embryo with photoactivatable fluorescence correlation spectroscopy, Nature communications*, 2013, **4**, 1637.
85. N. Plachta, T. Bollenbach, S. Pease, S. E. Fraser and P. Pantazis, *Oct4 kinetics predict cell lineage patterning in the early mammalian embryo, Nat Cell Biol*, 2011, **13**, 117-123.
86. N. Honkura, M. Matsuzaki, J. Noguchi, G. C. Ellis-Davies and H. Kasai, *The subspine organization of actin fibers regulates the structure and plasticity of dendritic spines, Neuron*, 2008, **57**, 719-729.
87. P. D. Calvert, W. E. Schiesser and E. N. Pugh, Jr., *Diffusion of a soluble protein, photoactivatable GFP, through a sensory cilium, J Gen Physiol*, 2010, **135**, 173-196.
88. M. Najafi, N. A. Maza and P. D. Calvert, *Steric volume exclusion sets soluble protein concentrations in photoreceptor sensory cilia, Proc Natl Acad Sci U S A*, 2012, **109**, 203-208.
89. Y. T. Kao, X. Zhu and W. Min, *Protein-flexibility mediated coupling between photoswitching kinetics and surrounding viscosity of a photochromic fluorescent protein, Proc Natl Acad Sci U S A*, 2012, **109**, 3220-3225.
90. M. Najafi, M. Haeri, B. E. Knox, W. E. Schiesser and P. D. Calvert, *Impact of signaling microcompartment geometry on GPCR dynamics in live retinal photoreceptors, J Gen Physiol*, 2012, **140**, 249-266.
91. A. Yildiz, J. N. Forkey, S. A. McKinney, T. Ha, Y. E. Goldman and P. R. Selvin, *Myosin V walks hand-over-hand: single fluorophore imaging with 1.5-nm localization, Science*, 2003, **300**, 2061-2065.
92. A. D. Douglass and R. D. Vale, *Single-molecule microscopy reveals plasma membrane microdomains created by protein-protein networks that exclude or trap signaling molecules in T cells, Cell*, 2005, **121**, 937-950.
93. Y. Teramura, J. Ichinose, H. Takagi, K. Nishida, T. Yanagida and Y. Sako, *Single-molecule analysis of epidermal growth factor binding on the surface of living cells, Embo J*, 2006, **25**, 4215-4222.
94. A. Kusumi, Y. Sako and M. Yamamoto, *Confined lateral diffusion of membrane receptors as studied by single particle tracking (nanovid microscopy). Effects of calcium-induced differentiation in cultured epithelial cells, Biophysical journal*, 1993, **65**, 2021-2040.
95. S. Manley, J. M. Gillette, G. H. Patterson, H. Shroff, H. F. Hess, E. Betzig and J. Lippincott-Schwartz, *High-density mapping of single-molecule trajectories with photoactivated localization microscopy, Nat Methods*, 2008, **5**, 155-157.
96. F. V. Subach, G. H. Patterson, M. Renz, J. Lippincott-Schwartz and V. V. Verkhusha, *Bright monomeric photoactivatable red fluorescent protein for two-color super-resolution sptPALM of live cells, Journal of the American Chemical Society*, 2010, **132**, 6481-6491.
97. R. M. Clegg, *Fluorescence resonance energy transfer, Curr Opin Biotechnol*, 1995, **6**, 103-110.
98. H. Wolf, B. G. Barisas, K. J. Dietz and T. Seidel, *Kaede for detection of protein oligomerization, Mol Plant*, 2013, **6**, 1453-1462.

99. O. M. Subach, D. Entenberg, J. S. Condeelis and V. V. Verkhusha, *A FRET-facilitated photoswitching using an orange fluorescent protein with the fast photoconversion kinetics, Journal of the American Chemical Society*, 2012, **134**, 14789-14799.
100. X. X. Zhou, H. K. Chung, A. J. Lam and M. Z. Lin, *Optical control of protein activity by fluorescent protein domains, Science*, 2012, **338**, 810-814.
101. A. B. Arrenberg, F. Del Bene and H. Baier, *Optical control of zebrafish behavior with halorhodopsin, Proc Natl Acad Sci U S A*, 2009, **106**, 17968-17973.
102. G. S. Baird, D. A. Zacharias and R. Y. Tsien, *Circular permutation and receptor insertion within green fluorescent proteins, Proc Natl Acad Sci U S A*, 1999, **96**, 11241-11246.
103. J. Nakai, M. Ohkura and K. Imoto, *A high signal-to-noise Ca(2+) probe composed of a single green fluorescent protein, Nat Biotechnol*, 2001, **19**, 137-141.
104. H. Hoi, T. Matsuda, T. Nagai and R. E. Campbell, *Highlightable Ca2+ indicators for live cell imaging, Journal of the American Chemical Society*, 2013, **135**, 46-49.
105. B. F. Fosque, Y. Sun, H. Dana, C. T. Yang, T. Ohyama, M. R. Tadross, R. Patel, M. Zlatic, D. S. Kim, M. B. Ahrens, V. Jayaraman, L. L. Looger and E. R. Schreiter, *Neural circuits. Labeling of active neural circuits in vivo with designed calcium integrators, Science*, 2015, **347**, 755-760.
106. A. T. Vessoni, A. R. Muotri and O. K. Okamoto, *Autophagy in stem cell maintenance and differentiation, Stem cells and development*, 2012, **21**, 513-520.
107. K. Jing and K. Lim, *Why is autophagy important in human diseases?, Experimental & molecular medicine*, 2012, **44**, 69-72.
108. D. W. Hailey and J. Lippincott-Schwartz, *Using photoactivatable proteins to monitor autophagosome lifetime, Methods in enzymology*, 2009, **452**, 25-45.
109. L. Esteban-Martinez and P. Boya, *Autophagic flux determination in vivo and ex vivo, Methods*, 2015, **75C**, 79-86.
110. D. W. Hailey, A. S. Rambold, P. Satpute-Krishnan, K. Mitra, R. Sougrat, P. K. Kim and J. Lippincott-Schwartz, *Mitochondria supply membranes for autophagosome biogenesis during starvation, Cell*, 2010, **141**, 656-667.
111. M. Tasaki, S. Asatsuma and K. Matsuoka, *Monitoring protein turnover during phosphate starvation-dependent autophagic degradation using a photoconvertible fluorescent protein aggregate in tobacco BY-2 cells, Frontiers in plant science*, 2014, **5**, 172.
112. J. Zhang, *Teaching the basics of autophagy and mitophagy to redox biologists-Mechanisms and experimental approaches, Redox biology*, 2015, **4C**, 242-259.
113. H. Koga, M. Martinez-Vicente, F. Macian, V. V. Verkhusha and A. M. Cuervo, *A photoconvertible fluorescent reporter to track chaperone-mediated autophagy, Nature communications*, 2011, **2**, 386.
114. M. Kon, R. Kiffin, H. Koga, J. Chapochnick, F. Macian, L. Varticovski and A. M. Cuervo, *Chaperone-mediated autophagy is required for tumor growth, Science translational medicine*, 2011, **3**, 109ra117.
115. L. Zhang, N. G. Gurskaya, E. M. Merzlyak, D. B. Staroverov, N. N. Mudrik, O. N. Samarkina, L. M. Vinokurov, S. Lukyanov and K. A. Lukyanov, *Method for real-time monitoring of protein degradation at the single cell level, Biotechniques*, 2007, **42**, 446, 448, 450.
116. K. H. Lodowski, R. Lee, P. Ropelewski, I. Nemet, G. Tian and Y. Imanishi, *Signals governing the trafficking and mistrafficking of a ciliary GPCR, rhodopsin, J Neurosci*, 2013, **33**, 13621-13638.
117. K. H. Lodowski and Y. Imanishi, *Monitoring of rhodopsin trafficking and mistrafficking in live photoreceptors, Methods Mol Biol*, 2015, **1271**, 293-307.
118. A. Poetsch, L. L. Molday and R. S. Molday, *The cGMP-gated channel and related glutamic acid-rich proteins interact with peripherin-2 at the rim region of rod photoreceptor disc membranes, J Biol Chem*, 2001, **276**, 48009-48016.

119. G. Tian, P. Ropelewski, I. Nemet, R. Lee, K. H. Lodowski and Y. Imanishi, *An unconventional secretory pathway mediates the cilia targeting of peripherin/rds, The Journal of neuroscience : the official journal of the Society for Neuroscience*, 2014, **34**, 992-1006.
120. L. M. Ritter, N. Khattree, B. Tam, O. L. Moritz, F. Schmitz and A. F. Goldberg, *In situ visualization of protein interactions in sensory neurons: glutamic acid-rich proteins (GARPs) play differential roles for photoreceptor outer segment scaffolding, The Journal of neuroscience : the official journal of the Society for Neuroscience*, 2011, **31**, 11231-11243.
121. T. K. Kerppola, *Bimolecular fluorescence complementation (BiFC) analysis as a probe of protein interactions in living cells, Annu Rev Biophys*, 2008, **37**, 465-487.
122. S. Karan, H. Zhang, S. Li, J. M. Frederick and W. Baehr, *A model for transport of membrane-associated phototransduction polypeptides in rod and cone photoreceptor inner segments, Vision Res*, 2008, **48**, 442-452.
123. J. Wang and D. Deretic, *Molecular complexes that direct rhodopsin transport to primary cilia, Prog Retin Eye Res*, 2014, **38**, 1-19.
124. I. Nemet, P. Ropelewski and Y. Imanishi, *Rhodopsin trafficking and mistrafficking: signals, molecular components, and mechanisms, Progress in molecular biology and translational science*, 2015.
125. K. Miyaguchi and P. H. Hashimoto, *Evidence for the transport of opsin in the connecting cilium and basal rod outer segment in rat retina: rapid-freeze, deep-etch and horseradish peroxidase labelling studies, J Neurocytol*, 1992, **21**, 449-457.
126. S. Obata and J. Usukura, *Morphogenesis of the photoreceptor outer segment during postnatal development in the mouse (BALB/c) retina, Cell Tissue Res*, 1992, **269**, 39-48.
127. J. Z. Chuang, Y. Zhao and C. H. Sung, *SARA-regulated vesicular targeting underlies formation of the light-sensing organelle in mammalian rods, Cell*, 2007, **130**, 535-547.
128. R. H. Steinberg, S. K. Fisher and D. H. Anderson, *Disc morphogenesis in vertebrate photoreceptors, J Comp Neurol*, 1980, **190**, 501-508.
129. I. Nemet, G. Tian and Y. Imanishi, *Organization of cGMP sensing structures on the rod photoreceptor outer segment plasma membrane, Channels*, 2014, **in press**.
130. R. S. Molday, D. Hicks and L. Molday, *Peripherin. A rim-specific membrane protein of rod outer segment discs, Invest Ophthalmol Vis Sci*, 1987, **28**, 50-61.
131. N. J. Cook, L. L. Molday, D. Reid, U. B. Kaupp and R. S. Molday, *The cGMP-gated channel of bovine rod photoreceptors is localized exclusively in the plasma membrane, J Biol Chem*, 1989, **264**, 6996-6999.
132. D. S. Williams, K. A. Linberg, D. K. Vaughan, R. N. Fariss and S. K. Fisher, *Disruption of microfilament organization and deregulation of disk membrane morphogenesis by cytochalasin D in rod and cone photoreceptors, The Journal of comparative neurology*, 1988, **272**, 161-176.
133. I. Nemet, G. Tian and Y. Imanishi, *Submembrane assembly and renewal of rod photoreceptor cGMP-gated channel: insight into the actin-dependent process of outer segment morphogenesis, J Neurosci*, 2014, **34**, 8164-8174.
134. M. A. Maw, D. Corbeil, J. Koch, A. Hellwig, J. C. Wilson-Wheeler, R. J. Bridges, G. Kumaramanickavel, S. John, D. Nancarrow, K. Roper, A. Weigmann, W. B. Huttner and M. J. Denton, *A frameshift mutation in prominin (mouse)-like 1 causes human retinal degeneration, Human molecular genetics*, 2000, **9**, 27-34.
135. A. Rattner, P. M. Smallwood, J. Williams, C. Cooke, A. Savchenko, A. Lyubarsky, E. N. Pugh and J. Nathans, *A photoreceptor-specific cadherin is essential for the structural integrity of the outer segment and for photoreceptor survival, Neuron*, 2001, **32**, 775-786.
136. Z. Yang, Y. Chen, C. Lillo, J. Chien, Z. Yu, M. Michaelides, M. Klein, K. A. Howes, Y. Li, Y. Kaminoh, H. Chen, C. Zhao, Y. T. Al-Sheikh, G. Karan, D. Corbeil, P. Escher, S. Kamaya, C. Li, S. Johnson, J.

M. Frederick, Y. Zhao, C. Wang, D. J. Cameron, W. B. Huttner, D. F. Schorderet, F. L. Munier, A. T. Moore, D. G. Birch, W. Baehr, D. M. Hunt, D. S. Williams and K. Zhang, *Mutant prominin 1 found in patients with macular degeneration disrupts photoreceptor disk morphogenesis in mice, The Journal of clinical investigation*, 2008, **118**, 2908-2916.

137. Z. Han, D. W. Anderson and D. S. Papermaster, *Prominin-1 localizes to the open rims of outer segment lamellae in Xenopus laevis rod and cone photoreceptors, Investigative ophthalmology & visual science*, 2012, **53**, 361-373.

138. A. Rattner, J. Chen and J. Nathans, *Proteolytic shedding of the extracellular domain of photoreceptor cadherin. Implications for outer segment assembly, J Biol Chem*, 2004, **279**, 42202-42210.

139. M. S. Kinney and S. K. Fisher, *The photoreceptors and pigment epithelium of the larval Xenopus retina: morphogenesis and outer segment renewal, Proceedings of the Royal Society of London. Series B, Containing papers of a Biological character. Royal Society*, 1978, **201**, 149-167.

140. M. Hofmann, C. Eggeling, S. Jakobs and S. W. Hell, *Breaking the diffraction barrier in fluorescence microscopy at low light intensities by using reversibly photoswitchable proteins, Proc Natl Acad Sci U S A*, 2005, **102**, 17565-17569.

141. T. Grotjohann, I. Testa, M. Leutenegger, H. Bock, N. T. Urban, F. Lavoie-Cardinal, K. I. Willig, C. Eggeling, S. Jakobs and S. W. Hell, *Diffraction-unlimited all-optical imaging and writing with a photochromic GFP, Nature*, 2011, **478**, 204-208.

142. P. Dedecker, G. C. Mo, T. Dertinger and J. Zhang, *Widely accessible method for superresolution fluorescence imaging of living systems, Proc Natl Acad Sci U S A*, 2012, **109**, 10909-10914.

143. T. Dertinger, R. Colyer, G. Iyer, S. Weiss and J. Enderlein, *Fast, background-free, 3D super-resolution optical fluctuation imaging (SOFI), Proc Natl Acad Sci U S A*, 2009, **106**, 22287-22292.

144. B. Moeyaert, N. Nguyen Bich, E. De Zitter, S. Rocha, K. Clays, H. Mizuno, L. van Meervelt, J. Hofkens and P. Dedecker, *Green-to-red photoconvertible Dronpa mutant for multimodal super-resolution fluorescence microscopy, ACS Nano*, 2014, **8**, 1664-1673.

145. C. H. Sung, C. Makino, D. Baylor and J. Nathans, *A rhodopsin gene mutation responsible for autosomal dominant retinitis pigmentosa results in a protein that is defective in localization to the photoreceptor outer segment, J Neurosci*, 1994, **14**, 5818-5833.

146. V. S. Lopes, D. Jimeno, K. Khanobdee, X. Song, B. Chen, S. Nusinowitz and D. S. Williams, *Dysfunction of heterotrimeric kinesin-2 in rod photoreceptor cells and the role of opsin mislocalization in rapid cell death, Molecular biology of the cell*, 2010, **21**, 4076-4088.

147. J. Mazelova, L. Astuto-Gribble, H. Inoue, B. M. Tam, E. Schonteich, R. Prekeris, O. L. Moritz, P. A. Randazzo and D. Deretic, *Ciliary targeting motif VxPx directs assembly of a trafficking module through Arf4, Embo J*, 2009, **28**, 183-192.

148. C. M. Louie, G. Caridi, V. S. Lopes, F. Brancati, A. Kispert, M. A. Lancaster, A. M. Schlossman, E. A. Otto, M. Leitges, H. J. Grone, I. Lopez, H. V. Gudiseva, J. F. O'Toole, E. Vallespin, R. Ayyagari, C. Ayuso, F. P. Cremers, A. I. den Hollander, R. K. Koenekoop, B. Dallapiccola, G. M. Ghiggeri, F. Hildebrandt, E. M. Valente, D. S. Williams and J. G. Gleeson, *AHI1 is required for photoreceptor outer segment development and is a modifier for retinal degeneration in nephronophthisis, Nature genetics*, 2010, **42**, 175-180.

149. T. Li, W. K. Snyder, J. E. Olsson and T. P. Dryja, *Transgenic mice carrying the dominant rhodopsin mutation P347S: evidence for defective vectorial transport of rhodopsin to the outer segments, Proc Natl Acad Sci U S A*, 1996, **93**, 14176-14181.

150. G. J. Pazour, S. A. Baker, J. A. Deane, D. G. Cole, B. L. Dickert, J. L. Rosenbaum, G. B. Witman and J. C. Besharse, *The intraflagellar transport protein, IFT88, is essential for vertebrate photoreceptor assembly and maintenance, The Journal of cell biology*, 2002, **157**, 103-113.

151. D. Shcherbo, E. M. Merzlyak, T. V. Chepurnykh, A. F. Fradkov, G. V. Ermakova, E. A. Solovieva, K. A. Lukyanov, E. A. Bogdanova, A. G. Zaraisky, S. Lukyanov and D. M. Chudakov, *Bright far-red fluorescent protein for whole-body imaging, Nat Methods*, 2007, **4**, 741-746.
152. P. K. Kim, D. W. Hailey, R. T. Mullen and J. Lippincott-Schwartz, *Ubiquitin signals autophagic degradation of cytosolic proteins and peroxisomes, Proc Natl Acad Sci U S A*, 2008, **105**, 20567-20574.
153. Y. Kabeya, N. Mizushima, T. Ueno, A. Yamamoto, T. Kirisako, T. Noda, E. Kominami, Y. Ohsumi and T. Yoshimori, *LC3, a mammalian homologue of yeast Apg8p, is localized in autophagosome membranes after processing, Embo J*, 2000, **19**, 5720-5728.
154. D. O. Wang, S. M. Kim, Y. Zhao, H. Hwang, S. K. Miura, W. S. Sossin and K. C. Martin, *Synapse- and stimulus-specific local translation during long-term neuronal plasticity, Science*, 2009, **324**, 1536-1540.
155. G. Tian, K. H. Lodowski, R. Lee and Y. Imanishi, *Retrograde intraciliary trafficking of opsin during the maintenance of cone-shaped photoreceptor outer segments of Xenopus laevis, J Comp Neurol*, 2014, **522**, 3577-3589.

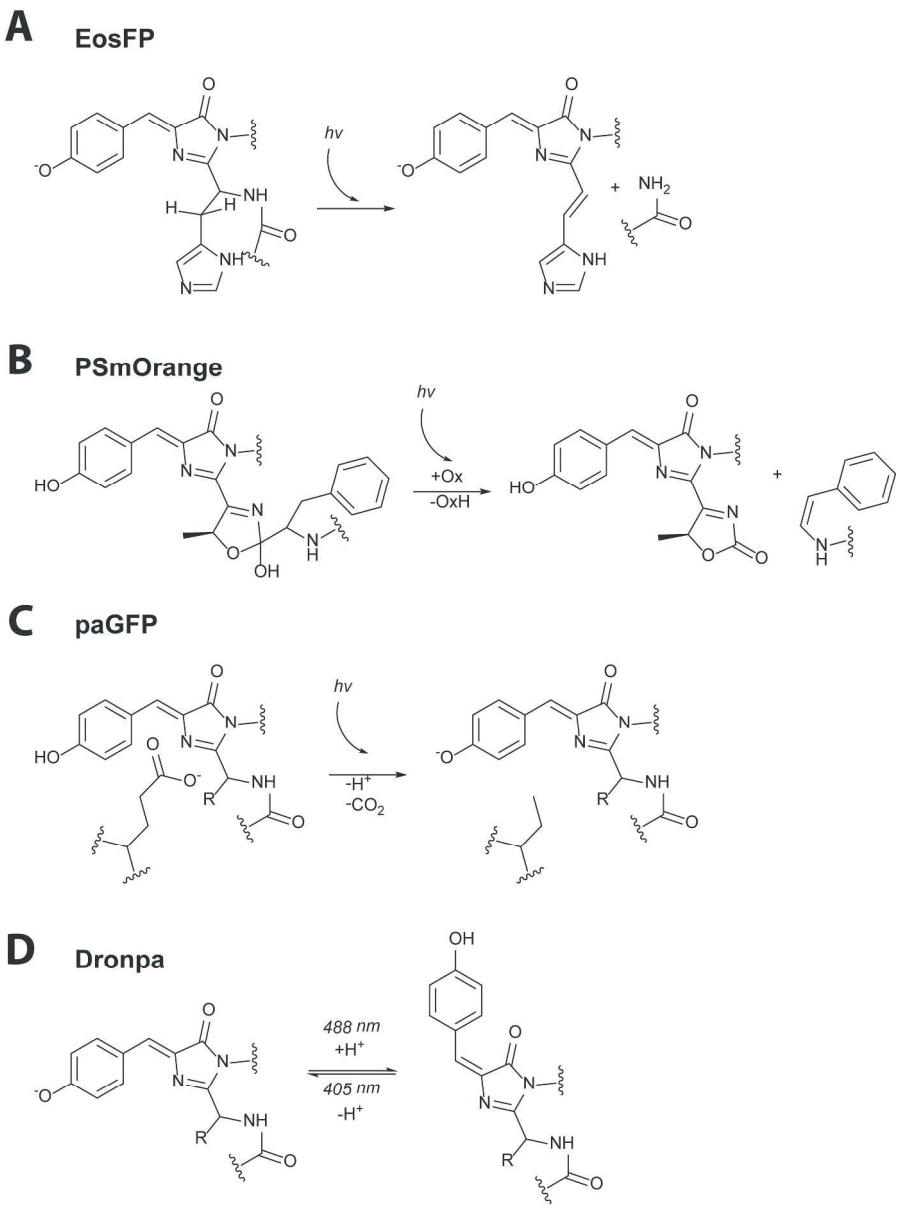

Figure 1. Light-induced chromophore transformations in phototransformable fluorescence proteins (PtFPs). Examples of irreversibly photoconvertible fluorescent proteins (EosFP and PSmOrange) (A,B), photoactivatable green fluorescent protein (paGFP) (C), and photoswitchable fluorescence protein (Dronpa) (D). Ox, oxidant molecule; OxH, reduced oxidant molecule; hv, irradiation with light.
228x307mm (300 x 300 DPI)

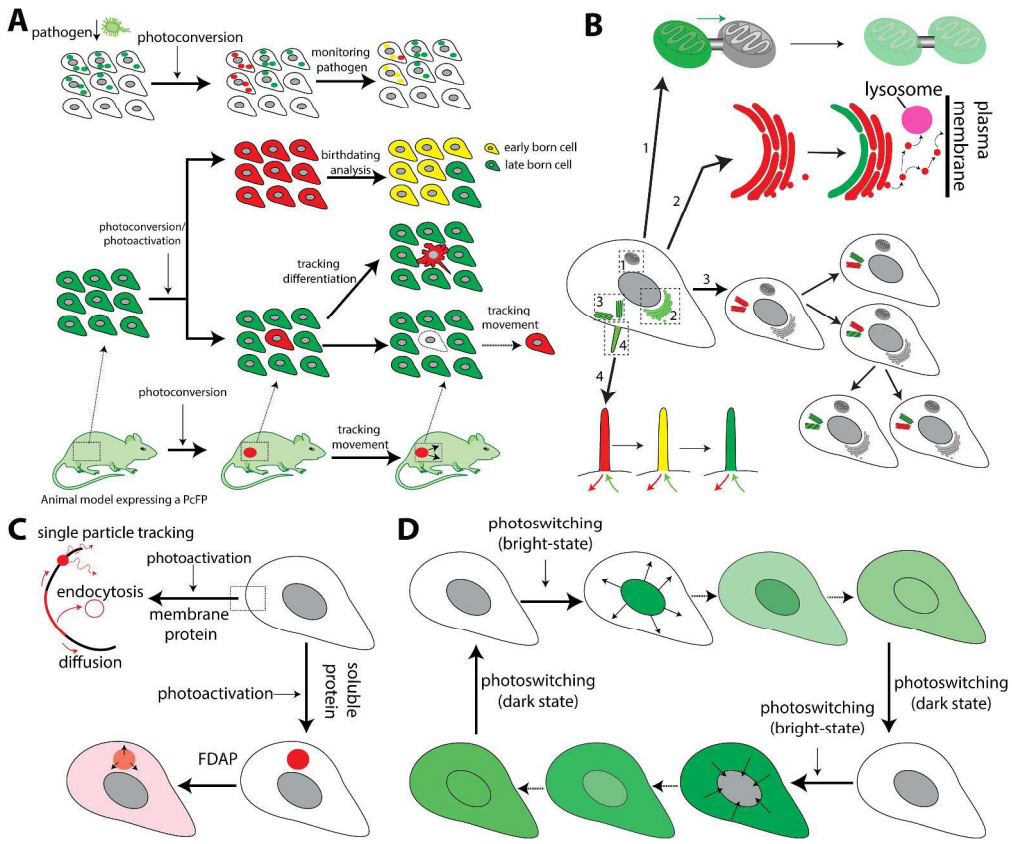

Figure 2. Application of PtFPs in visualizing biological processes. (A) Tracking of cell movement and differentiation, determination of cells' birthdates, and monitoring of metabolism in pathogens. After photoconversion/photoactivation, individual cells can be distinguished from their surrounding and monitored over time. (B) PaFPs and PcFPs were used to study mitochondria interactions (1); Golgi dynamics and secretory pathway (2); inheritance pattern of centrioles (3) and exchange of signaling components in cilia (4). (C) Models of monitoring protein diffusion by fluorescence decay after photoactivation (FDAP), monitoring membrane protein endocytosis, and tracking single particle. (D) Visualization of protein translocation by PsFPs.
426x356mm (300 x 300 DPI)

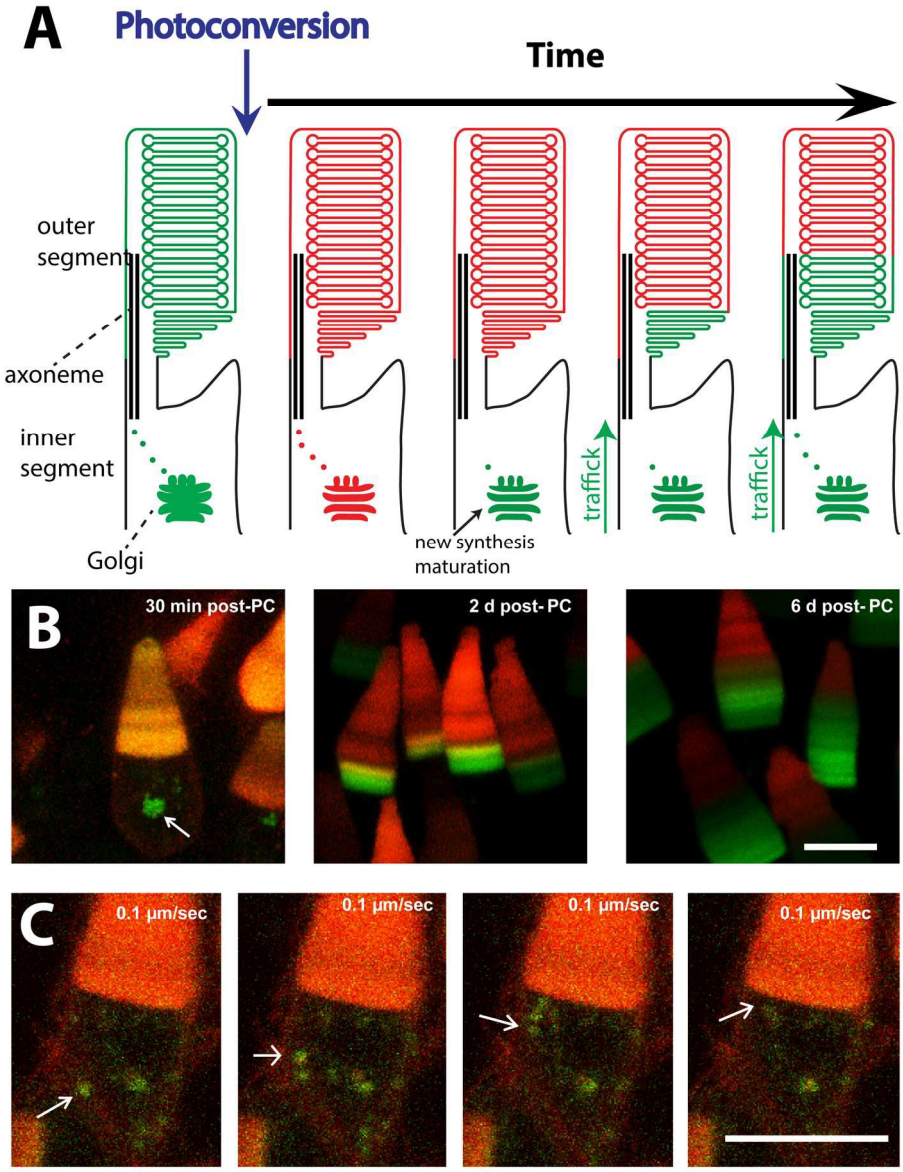

Figure 3. Application of the PcFP Dendra2 for imaging of rhodopsin trafficking in live Xenopus laevis rod photoreceptor cells. (A) Schematic representation of the photoconversion (PC) technique. Rhodopsin fused to Dendra2 (rhodopsin-Dendra2) is green prior to PC, and is switched to red after PC. New rhodopsin-Dendra2 (green) is synthetized in the inner segment and trafficked to the outer segment where it gets incorporated into disks. (B, C) Live Xenopus laevis rod photoreceptor cells expressing rhodopsin-Dendra2. Newly synthetized rhodopsin-Dendra2 can be observed in the inner segment shortly after PC (B, left panel, arrow); Rod outer segments are renewed over days (B, middle and right panel). (C) Vesicles containing newly synthetized rhodopsin-Dendra2 can be seen moving from the inner toward the outer segment. Images are maximum projections of optical slices. Scale bars, 10 µm. Images in (B) and (C) were adopted from Lodowski et al.116
164x200mm (300 x 300 DPI)

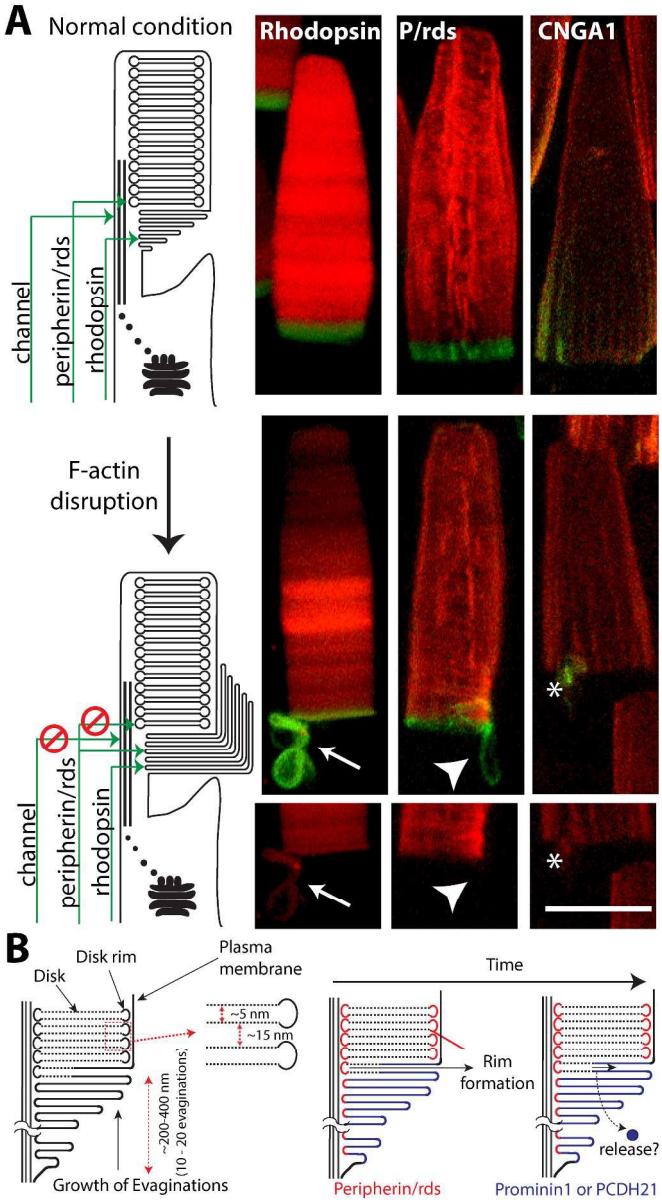

Figure 4. Application of PcFP Dendra2 for monitoring photoreceptor outer segment morphogenesis. Under normal conditions newly synthetized (green) rhodopsin-Dendra2 is incorporated into the evaginations, peripherin/rds-Dendra2 into the disk rim region, and cGMP gated channel (CNGA1-Dendra2) into the plasma membrane (A, upper row). When F-actin is disrupted, disks fail to mature and precursors of disks (evaginations) overgrow (A, middle and bottom row). Overgrown evaginations contain preexisting (red) and newly added rhodopsin-Dendra2 (green) (A, middle and bottom rows, arrows) and only newly synthetized peripherin/rds-Dendra2 (A, middle and bottom rows, arrow heads). In the absence of disk formation, CNGA1-Dendra2 cannot enter the outer segment (A, middle row, asterisk). Images are maximum projections of optical slices. The top panel of CNGA1 was adapted from Nemet et al.133 Scale bars, 10 μm. (B) A model describing rod disk membrane morphogenesis. In this model, evaginations grow gradually at the base of the outer segment. The growth accompanies with accommodation of PCDH21 and prominin-1 which facilitate the formation of membrane protrusion. After complete growth of evagination, rim region of disk is formed, leading to accommodation of peripherin/rds, expulsion of prominin-1 and proteolysis of

PCDH21. Rim formation coincides with sealing of evagination and separation of disk from the plasma membrane.
234x429mm (300 x 300 DPI)

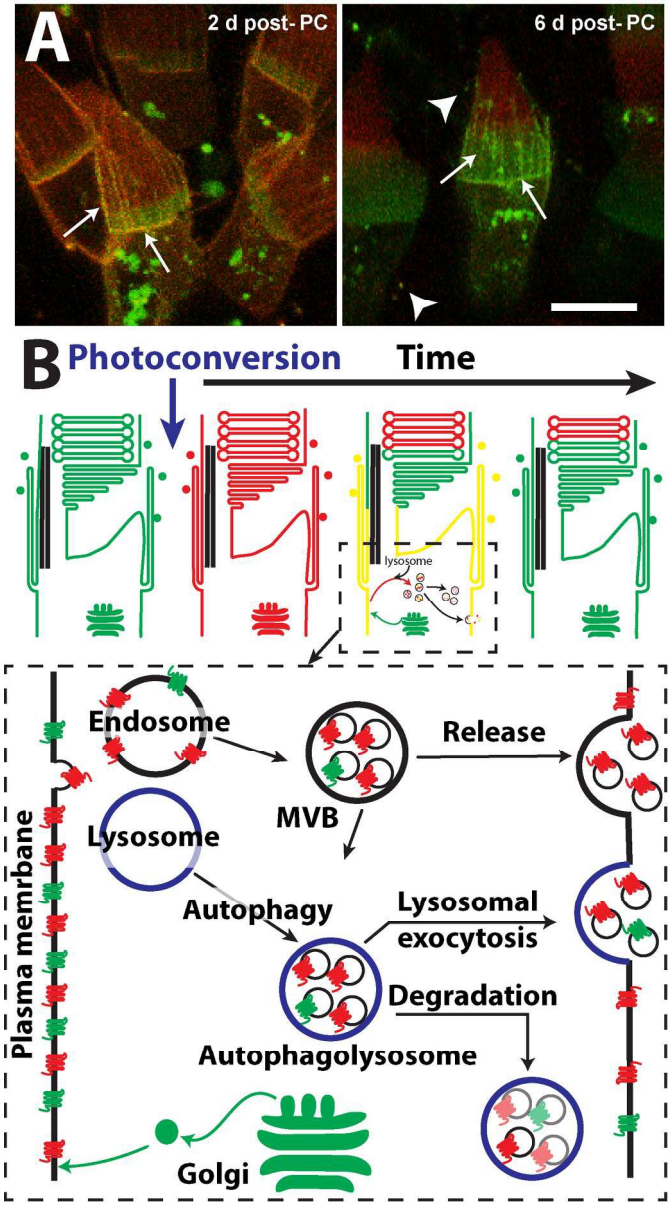

Figure 5. Monitoring removal of mislocalized mutant rhodopsin (Q344ter) in live Xenopus laevis rod photoreceptor cells. (A) RhodopsinQ344ter-Dendra2 mislocalizes to the inner segment plasma membrane including calyceal processes (arrows). Over time mislocalized rhodopsin is renewed at the plasma membrane (arrows). At 2 days post photoconversion (2 d post-PC), the plasma membrane is yellow because it is occupied with both old (red) and new (green) RhodopsinQ344ter-Dendra2. At 6 days post photoconversion (6 d post-PC), old RhodopsinQ344ter-Dendra2 was removed and new RhodopsinQ344ter-Dendra2 was added, resulting in green fluorescent plasma membrane. Images are maximum projections of confocal sections, and were adopted from Lodowski et al.116 Scale bar, 10 μm. (B) Schematic representations of hypothetical mechanisms involved in removal of mislocalized rhodopsin, and how a green-to-red PcFP can be used unravel those mechanisms. MVB stands for multivesicular body.
139x252mm (300 x 300 DPI)

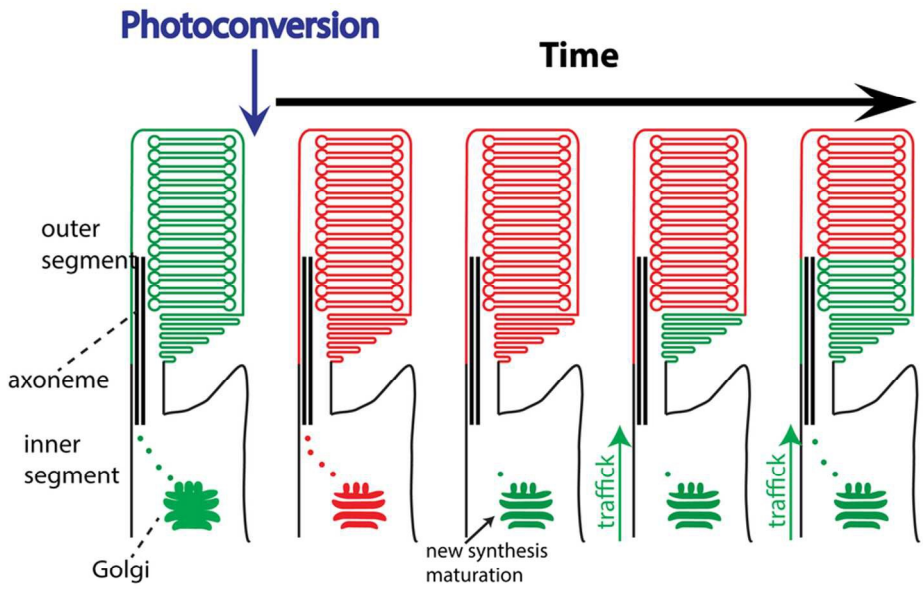

Phototransformable fluorescent proteins are GFP orthologs whose emission and excitation properties are modulatable by light. These reporter proteins give specific advantages to study protein trafficking in a spatiotemporal manner.
88x58mm (300 x 300 DPI)